THE SOURCE AND MAGNITUDE OF SUBMARINE GROUNDWATER DISCHARGE ALONG THE KONA COAST OF THE BIG ISLAND, HAWAII

THESIS SUBMITTED TO THE GRADUATE DIVISION OF THE UNIVERSITY OF HAWAIʻI IN PARTIAL FULFILLMENT OF THE REQUIREMENTS FOR THE DEGREE OF

MASTER OF SCIENCE

IN

GEOLOGY AND GEOPHYSICS

AUGUST 2018

By

Catherine Y. Hudson

Thesis Committee

Henrietta Dulai, Chair
Aly El-Kadi
Nicole Lautze

Abstract:

Submarine groundwater discharge (SGD) is present along the coastline where freshwater flows from the land, combines with brackish water circulation, and enters the sea. The purpose of this study is to quantify SGD along the shoreline and to identify the origin of the groundwater in SGD in the Hualalai aquifers on the Kona Coast of the Big Island, Hawaii. We collected SGD samples at coastal springs spanning along 82 km of shoreline of the combined Kiholo and Keauhou aquifers, and then analyzed samples to determine their oxygen isotope values. The stable oxygen isotopes of water trend to more negative values with increasing duration and altitude of precipitation and were therefore used to predict recharge elevation. After determining the oxygen isotopic composition of samples, we calculated the expected oxygen isotopic composition of precipitation in the form of snow, rain, or fog drip. As an approximation, it is assumed that such values are applicable to infiltrated water that percolates through permeable rock to enter the subsurface aquifer. By performing this calculation at increasing distances upslope along assumed flow paths, the elevation of SGD recharge was determined based on the integrated recharge isotopic signature. After identifying this elevation, we then projected possible groundwater areas of recharge to the points of discharge at the coastline. While the exact flow paths cannot be determined using this method, we identified five separate possible water recharge regions within the two aquifers, some which span outside of the aquifer boundaries. In the north Kiholo Aquifer, the water mass balance of SGD discharge-recharge volume within north Kona suggest that only about 37% of water originates from recharge within the Kiholo Aquifer boundary. Findings also suggest that, despite geological barriers, SGD signatures are very similar across the Kiholo-Keauhou boundary,

implying similar recharge areas and flow paths. In Keauhou aquifer, recharge to the basal lens makes up only 9-39% of SGD. The rest of the water is sourced from the high-level aquifer. In the case of south Keauhou Aquifer, SGD signatures suggest significant recharge contributions from elevations beyond the aquifer boundary. This study concludes that there are complex recharge and flow patterns in the Hualalai aquifers, suggesting recharge contributions from neighboring upstream aquifers and the occurrence of lateral flow to adjacent neighboring aquifers. This study was not able to quantify the exact recharge-discharge water balance due to missing SGD values in the south Keauhou aquifer. It was also not able to directly quantify, only imply, that some recharge is channeled to deeper aquifer layers, perhaps discharging farther offshore. Nevertheless, the study confirmed past findings and provided new insights into the interconnectivity of the aquifers in the Hualalai region.

Table of Contents

LIST OF TABLES

LIST OF FIGURES

Chapter 1. The Source and Magnitude of Submarine Groundwater Discharge Along the Kona Coast of the Big Island, Hawaii

Introduction:

Submarine groundwater discharge (SGD) is present along parts of the coastline where fresh and brackish groundwater flow from the land and enter the sea (Burnett and Dualiova, 2003; Sawyer et al., 2016). Groundwater can enter the ocean either via discreet springs or as diffuse seepage along a length of coastline, but usually it is a mixture of these outflows (Johnson, 2008; Peterson et al., 2009). Fresh SGD is driven by the hydraulic gradient between the coastal aquifer and the ocean. The quantity of groundwater that discharges to the coastal ocean therefore depends on a variety of terrestrial and marine factors. Terrestrial factors include the amount of precipitation that recharges the aquifer, permeability of the aquifer, and other water in- and outputs in the form of groundwater withdrawal, irrigation, or injection. Marine factors including waves, currents, density, and tidal action can also affect the saline flux of SGD into the coastal aquifer (Knee et al., 2008; Dulai et al., 2015).

Historically, streams and rivers have been studied more excessively than SGD and in many places globally SGD remains unquantified. This is largely due to the difficulty in detecting

and measuring submarine discharge. The first comprehensive methods to study SGD were performed in parallel by Moore (1996) and Cable et al. (1996). These studies recognized and defined SGD and focused on methods to not just detect, but also quantify discharge. The few studies that have looked at SGD on larger scales have determined that SGD water and nutrient inputs into oceans are often greater than riverine inputs (Kwon et al., 2014). This same pattern also holds true for SGD in Hawaii, where it has been previously hypothesized that groundwater fluxes to Hawaii's coastal waters can be greater than the amounts of water added by streams and rivers over land (Knee et al., 2008, Dulai et al., 2016). Water quality in SGD can depend on many human and natural influences, including pumping rates that can lead to saltwater intrusion and chemical inputs (which can elevate nutrient levels), as well as non-anthropogenic factors such as the chemical weathering of rocks (Moore, 1998; Johnson et al., 2008; Peterson et al., 2009; Knee et al., 2010; Sawyer et al., 2016). SGD is therefore significant for water as well as nutrient budgets locally and globally.

SGD plays a significant role in the water cycle because it is part of the water budget of every coastal watershed. SGD measurements can therefore help improve the characterization of water budgets and water resources. This study focuses on SGD along the Kona coast of the Big Island, Hawaii and specifically looks at the two aquifers that encompass Hualalai Mountain: Kiholo Aquifer in the north and Keauhou Aquifer in the south (Figure 1.1). These two aquifers were chosen due to the limited understanding of their subsurface hydrogeology and the hypothesis that there are subsurface structures in this region that influence the transport, residence time, storage, and potential contamination of groundwater (Oki, 1999; Bauer, 2003; Tillman et al., 2014; Ike Wai Project Description, 2015). Studying coastal SGD in these aquifers has the potential to help better characterize groundwater flow paths and aquifer

interconnectivity based on the magnitude and location of SGD along the coast. In turn, this will help improve our understanding of the water budget for this area and can assist with planning to ensure West Hawaii's water security in the future. This is of particular importance because the Kona area is entirely dependent on groundwater for all anthropogenic or agricultural purposes due to the lack of streams or other surface water. With a changing climate causing disruptions to rainfall patterns and aquifer recharge, and an increasing population and growing tourism industry, it is more important than ever to understand West Hawaii's water budget to help assist with future water planning and security (Gregg et al., 2004).

Previous research done by Johnson (2008), Street et al. (2008), Peterson et al. (2009), Knee et al. (2010), and Waters (2015) located SGD plumes along the Kona coastline using thermal infrared (TIR) imaging and geochemical tracers. But although the major locations of discharge have been identified and quantified, the role of SGD as a component of the water balance, including the amount of discharge compared to recharge and the origin of the groundwater, i.e. the area where precipitation in the form of rainfall, snow, hail, vog (volcanic smog) drip, or fog drip enters the aquifer, is still not well understood. Such characterization of recharge locations may help improve understanding of groundwater flow paths and the interconnectivity of the aquifers.

From the perspective of water resources, SGD is also important in specific yield determinations. Excessive groundwater withdrawals cause seawater intrusion, which has been the primary concern of water managers, but recently it has been shown to lead to decreased stream base flow and SGD (Oki 1999). SGD is an important driver of coastal water quality as well as a source of nutrients to the reef and coastal ponds. Many studies have confirmed that

SGD is often a delivery pathway that carries nutrients to the coastal ocean (Slomp et al., 2004; Duarte et al., 2006; Johnson et al., 2008; Glenn et al., 2013; Nelson et al., 2015; Amato et al., 2016; Knee et al., 2016; Prouty et al., 2017). Nutrients are an important part of the coastal ecosystem and promote algal growth that sustains a healthy coral reef and the nearshore community (Hoover and MacKenzie, 2009). That being said, too many nutrients cause harmful algal blooms that lower the oxygen content of the water and cause eutrophication, in turn leading to dead zones that can kill fish and other animals in the community (Amato et al., 2016). As a prominent pathway for nutrient delivery to coastal waters, SGD studies are necessary to determine where the water and its associated nutrients originate, as well as how this pathway may be affected by changes in recharge and/or groundwater withdrawals.

Previous researchers attempted to characterize water flow paths, ages of water masses, and source areas of groundwater recharge by sampling groundwater from wells and coastal ponds that are located in Kona. These studies used stable isotopes of water and geologic information to derive recharge elevations and possible groundwater flow paths (Tillman et al. 2014; Kelly and Glenn, 2015; Fackrell, 2016). These studies found that groundwater in the West Hawaii study area tends to originate from the upper regions of Mauna Kea and Mauna Loa as opposed to the flanks of the lower Hualalai Mountain (Tillman et al., 2014; Fakcrell, 2016). They also confirm that fog drip contributes to aquifer recharge, and that high water-level and basal lens aquifers are interconnected (Tillman et al., 2014; Kelly and Glenn, 2015). Although these studies greatly improved our current knowledge concerning the origin of the groundwater, they were performed at set locations defined by well locations and depths, and are limited in number. Therefore, there is still relatively little that is known about aquifer catchment areas and recharge elevations.

This research takes advantage of the numerous and relatively evenly distributed groundwater discharge outcrops along the coastline and builds on previous studies by using the established stable isotope and recharge elevation relationship defined by Scholl et al. (1996) and Fackrell (2016). This study aims to delineate the lateral extent of groundwater masses of similar origin and their recharge zones upslope of the discharge points. It will also compare water recharge and discharge rates for these defined catchment areas to see if SGD at the coastline accounts for all of the upslope recharge in West Hawaii. By comparing recharge and discharge rates, we will be able to have a better understanding of water budgets in individual portions of the aquifer.

There are four main objectives of this study: 1) utilizing previous research complemented by additional measurements, determine the flux of nearshore SGD at the coast for two of the Big Island's major aquifers: Kiholo in the North and Keauhou in the South, 2) identify the source of the coastal aquifer water based on the chemical composition of groundwater springs and delineate groups with similar groundwater composition, 3) determine the catchment areas for each group of springs by looking at possible flow pathways determined from groundwater recharge elevations, and 4) compare the nearshore fresh SGD to the amount of recharge for each group to see if there are other factors (geologic or anthropogenic) that may redirect groundwater to deeper layers or laterally as inter-aquifer flow. Accomplishing these goals will help improve our understanding of the water budget for this area and can assist with planning to ensure West Hawaii's water security in the future.

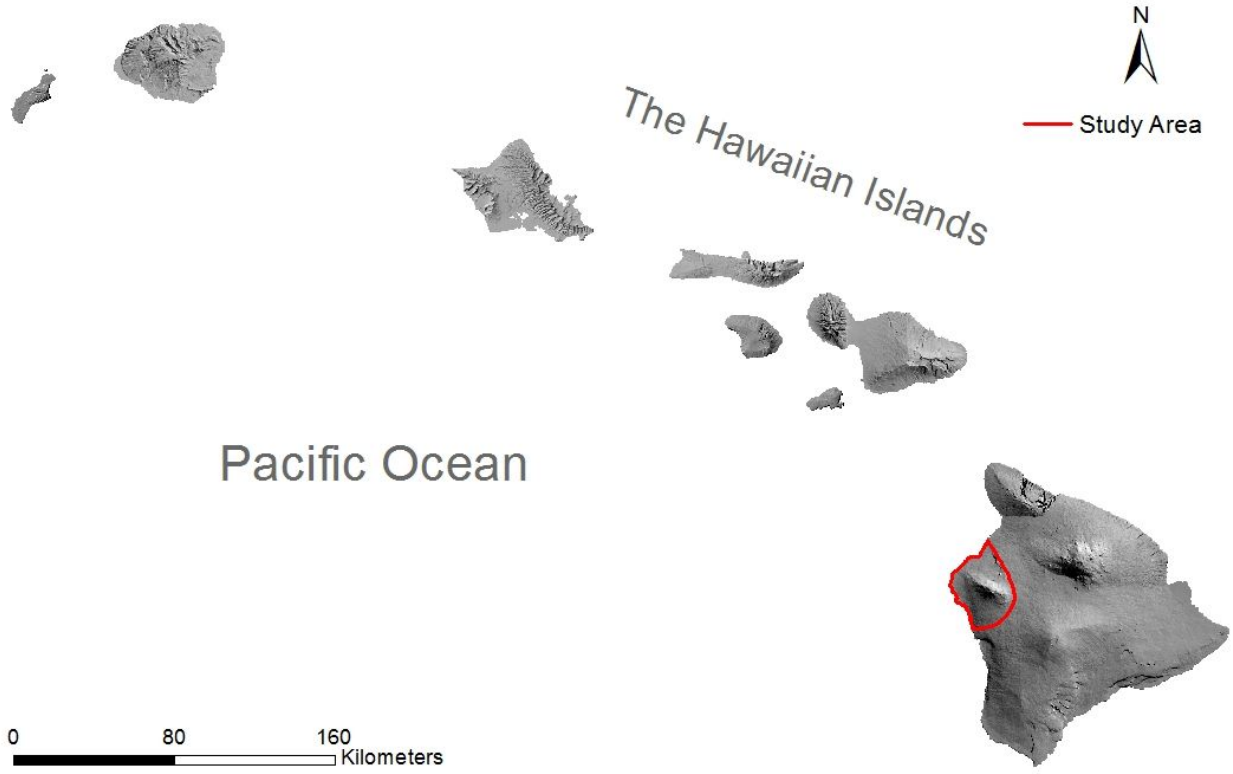

Figure 1.1 Map of the Hawaiian Island chain with the study area outlined in red. Hillshade model from NOAA, 2007.

Background:

Climate and Rainfall of West Hawaii

Despite an average rainfall of 263.1 mm in Kiholo Bay, 498.9 mm in Honokohau Harbor, and 685.0 mm in downtown Kona annually, there are no perennial streams located on the Kona Coast (Giambelluca et al., 2014). Therefore, surface runoff was not taken into consideration in

this study. Instead, water seeps through the volcanic basalt and into the aquifer located under the land surface. This freshwater aquifer is currently the main source of domestic water in the Kona area and is pumped at a rate of 89,177 m^3/d for the combined Hualalai aquifers (Commission On Water Resources Management, unpublished data, 2017). Once underground, the water does not stay in the aquifer permanently. Instead, similar to above ground streams and rivers, it flows underground and discharges into the ocean. This submarine groundwater discharge is unique from seawater in that it has a lower salinity, colder temperature, and a different chemical signature that distinguishes it from seawater.

A temperature inversion boundary layer, above which the trade wind clouds evaporate, occurs at roughly 2000m above sea level and is a consistent feature of the trade wind pattern that occurs on the Big Island of Hawaii. This boundary is caused by air temperatures that briefly rise, causing a cool layer of air at the surface that is overlain by warmer air, before the air temperature continues to decrease with increasing altitude in the atmosphere. (Scholl et al., 1996). Above this boundary mountainous rainfall is uncommon. Instead, the majority of precipitation originates from infrequent low pressure systems known as “Kona storms”, though some recharge can also originate from fog drip at this elevation (Scholl et al., 1996; Engott, 2011; Kelly and Glenn, 2015; Fackrell, 2016).

Because Kona is located on the leeward side of the island and is in the rain shadow of Mauna Loa and Mauna Kea, it would typically be assumed to have more depleted water isotopes due to rainout as the vapor journeys from the windward to the leeward side. Instead, it has been observed that water vapor that contributes to the Kona area originates from the leeward side of the Big Island and is pushed over land by daily sea breezes before condensing and precipitating (Fackrell, 2016). This causes the stable isotopes of water (^2H and ^{18}O) to

become more depleted at a predictable rate as the water vapor condenses and precipitates as it moves inland (Scholl et al., 1996; Scholl et al., 2002; Fackrell, 2016).

It has been observed that water vapor that contributes to the Kona area is sourced from the leeward side of the Big Island, where lower atmospheric humidity results in a higher humidity gradient across the air-sea interface. As a result, deuterium (δ^2H) experiences greater kinetic fractionation than oxygen (Fackrell, 2016). Therefore, this study focuses on the oxygen isotopic values collected from each sampling site because the measured values should more closely match the isotopic values of recharge for this area. It was assumed that the measured $\delta^{18}O$ isotopes reflected the $\delta^{18}O$ isotopes of recharge for this study area, with no fractionation occurring due to evaporation or photosynthesis (Fackrell, 2016), though recent findings by Dudley et al. (in prep) suggest a minimal fractionation of ~1.5‰ during this process.

On top of rainfall, fog and vog are important factors to consider when discussing isotopic signatures of precipitation. Though there is limited research involving vog drip, fog drip is known to be isotopically enriched compared to rainfall (Scholl et al., 2002). In West Hawaii, the fog drip boundary tends to run between 975m and 2255m (Kelly and Glenn, 2015). Unfortunately, no fog drip collection studies have been performed in the West Hawaii study area, so it is unclear how much influence these components have on the isotopic composition of precipitation. Though fog drip has been shown to contribute to aquifer recharge (Oki, 1999; Engott, 2011; Kelly and Glenn, 2015).

Geology and General Land Cover of West Hawaii

The Big Island is composed of five shield volcanoes: Hualalai, Mauna Kea, Mauna Loa, Kohala and Kilauea (Clague and Langenheim, 1987; Prouty et al., 2017). This study focuses on the first three, of which Mauna Kea is to the north, Mauna Loa to the south, and Hualalai, which is encompassed by the study area, located to the west (Figure 1.2).

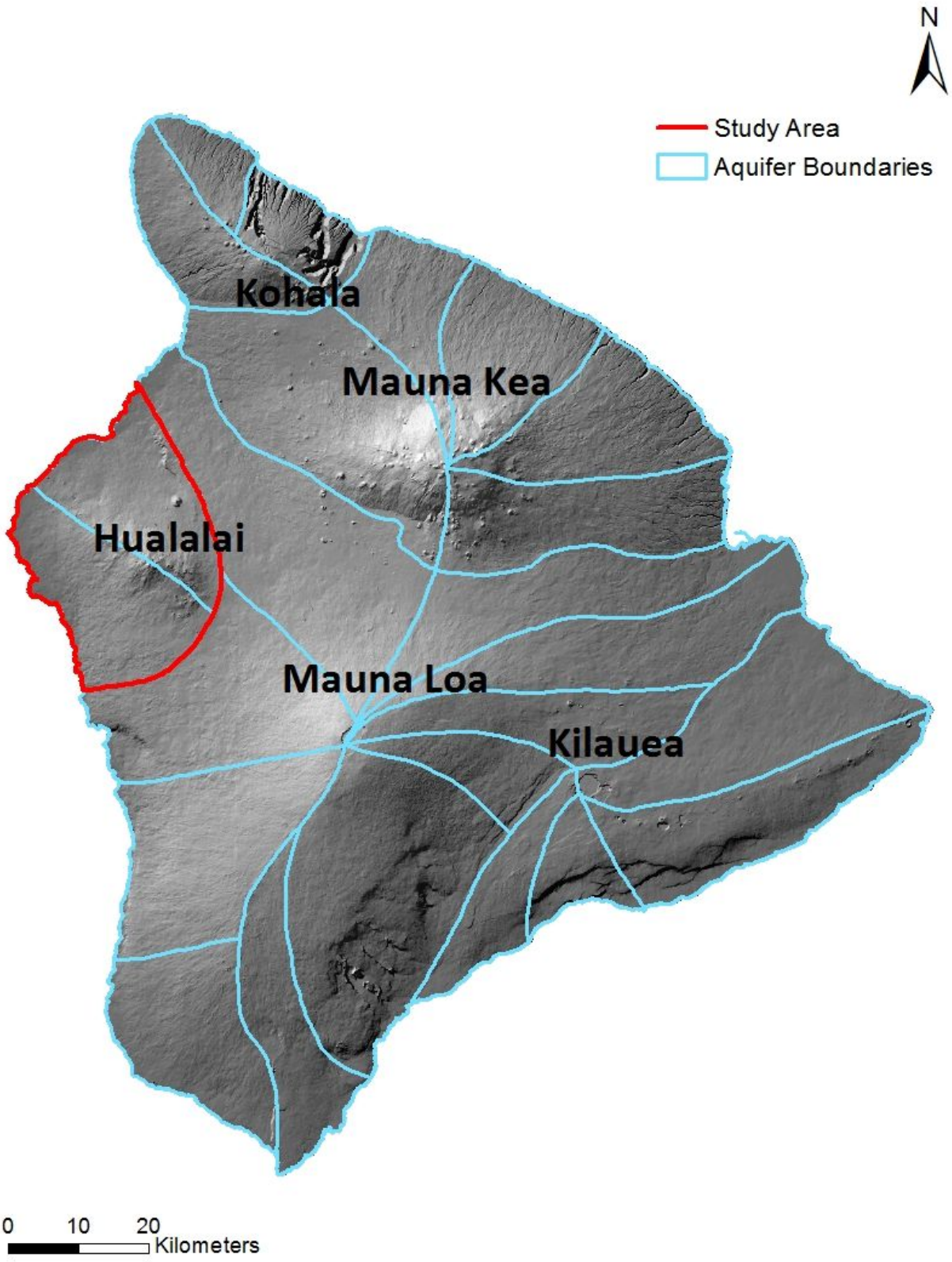

Figure 1.2 Map of the Big Island with each of the five shield volcanoes labeled, aquifer boundaries outlines are in blue, and the study area is outlined in red. Hillshade model from NOAA, 2007.

The samples collected in this study surround the flanks of the Hualalai volcano, which rises to a height of 2,523m and is largely composed of unexposed tholeiitic basalt thinly capped by a layer of alkalic basalt (Moore et al., 1987). The alkalic lava on its northern, eastern, and southern flanks is also interbedded with tholeiitic lava sourced from Mauna Loa (Moore et al., 1987).

Mauna Loa has erupted 39 times since 1832 (Gregg et al., 2004). Since that time, 7 lava flows have entered the Kona area, the most recent flow taking place in 1950 and skirting the northern edge of Hualalai (Gregg et al., 2004). Several lava flows from Hualalai lead both north and south of the summit and occurred near 1800, though these flows are not as well documented (Gregg et al., 2004; Tillery and El-Kadi, 2012). Current lava flows follow topography and appear unaffected by subsurface structures.

Hualalai has one known rift zone that strikes north-northwest along the aquifer boundary line. There are two other subsurface structures, one that strikes north and another that strikes south-southeast, that are thought to be rift zones as well, though this is still being researched (Stearns and MacDonald, 1946; Adams et al., 1971; Tillery and El-Kadi, 2012). Each of these subsurface structures, whether they are rift zones or remain unidentified subsurface structures, begins at a point roughly 5km to the east of the summit of Hualalai (Moore et al., 1987). Another structure identified by Adams (1971) runs from the northwest flank of Mauna Kea downslope and westward toward the Kiholo Bay area, which could present a potential direct path for groundwater flow. Trachyte, rich in SiO_2, also appears on the north rift zone of Hualalai at the Puu Waawaa cone (Peterson and Moore, 1987; Tillery and El-Kadi, 2012).

Structures such as fractures, faults, dikes, and lava tubes can exert significant influence over the path and residence time of groundwater in the aquifer. Dikes are typically associated with rift zones and are low-permeability and low-conductivity structures that tend to impound the groundwater, therefore extending its residence time (Tillery and El-Kadi, 2012; Kelly and Glenn, 2015). These dike structures can extend vertically and laterally for a few kilometers (Oki, 1999; Kelly and Glenn, 2015). Though, it should be noted that these structures can keep some water from leaking across the dike boundaries (Tillery and El-Kadi, 2012). On the other hand, lava tubes exhibit high hydraulic conductivity and can provide a direct pathway for groundwater, in turn shortening residence time in the aquifer (Kelly and Glenn, 2015).

The majority of the Hualalai study area is comprised of bare exposed rock, specifically along the coastline of Kiholo Aquifer and near the summit of the Hualalai (1976 Digital GIRAS files, Hawaii Statewide GIS Program). Further inland, Kiholo Aquifer land use ranges from grassland at lower elevations to shrubland at higher elevations, also including an area of native forest (Tillery and El-Kadi, 2012). Keauhou Aquifer, containing Kona town, is mostly comprised of rangeland or urban areas with only a little bare rock, though there is some grassland and small scatterings of forest cover and shrubland further inland (1976 Digital GIRAS files, Hawaii Statewide GIS Program; Tillery and El-Kadi, 2012). Keauhou also contains the Kealakahe Wastewater Treatment Plant, which disposes of effluent in a drainage pit further inland near the highway (Oki, 1999; Tillery and El-Kadi, 2012). This effluent is thought to contribute nutrients to SGD, specifically around Honokohau Harbor (Johnson et al., 2008; Hunt, 2008; Waters, 2015). Keauhou is more urbanized than Kiholo, as it contains the town of Kailua-Kona. It should be noted that the entire study area is becoming more urbanized given the rise in

tourism and population in recent years, particularly with the additions of resorts in Kiholo (Gregg et al., 2004).

Groundwater

In the Kona area, recharge, be it from rainfall, fog drip, hail, or snow seeps through the highly permeable volcanic basalt and into the aquifer located under the land surface (Stearns and MacDonald, 1946; Scholl et al., 1996; Kelly and Glenn, 2015; Fackrell, 2016). Once in the aquifer, the less dense freshwater that originated from above ground "floats" on top of the more dense seawater and creates a freshwater lens according to Ghyben-Herzberg principles. Once in the aquifer, the fresh groundwater may be extracted in the form of pumping for agricultural or anthropogenic usage, depleting this resource.

The groundwater in the Kona area exists as a thin basal lens at the coast and extends inland for several kilometers (Oki, 1999). In the Keauhou Aquifer, the groundwater has been found at significantly higher head levels at wells drilled further inland (Oki, 1999; Bauer, 2003; Kelly and Glenn, 2015; Fackrell, 2016). Low water levels closer to the coast are generally less than 10ft above sea level while well water levels further inland are generally 25-500ft above sea level (Oki, 1999; Bauer, 2003). This divide occurs at roughly 250-550m elevation on the flanks of Hualalai and it is currently unknown what type of structures have trapped the groundwater at such high levels and exactly where they occur (Figure 1.3). That being said, it has been hypothesized that a buried dike complex, impermeable flows such as ash layers or a dense sequence of lava flows, or faulting later buried by lava flows may be responsible for the high

head levels (Oki, 1999; Bauer, 2003; Tillery and El-Kadi, 2012; Tillman et al., 2014; Kelly and Glenn, 2015; Fackrell, 2016).

Although these structures have not been characterized, they would be expected to exert an enormous amount of influence over the groundwater flow and residence time in West Hawaii. Aquifers at higher elevations above the water-level divide are referred to as high-level due to the elevated water levels in their wells (Kelly and Glenn, 2015). Groundwater located in the high-level aquifer may become isolated and compartmentalized, in turn creating slightly leaky groundwater reservoirs that flow parallel to the subsurface structures or leak into the basal lens (Scholl et al., 1996; Kelly and Glenn, 2015). In the high-level aquifer, the impermeable layers isolate the water, and oxygen and hydrogen isotopes of the groundwater and precipitation in the area suggest that recharge into the high-level aquifer contributes to groundwater recharge in the basal lens, though this is still being researched and debated (Oki, 1999; Fackrell and Glenn, 2014; Tillman, 2014; Kelly and Glenn, 2015).

Kelly and Glenn, 2015 used chlorofluorocarbon (CFC) age dating to determine that groundwater in the high-level area of the aquifer is largely comprised of “old” groundwater that entered the system prior to 1940 while the basal lens contains mostly “young” groundwater that entered the aquifer as recharge after 1940. These samples were collected from drinking supply wells, brackish coastal ponds, coastal monitoring wells, and one lava tube at 18 locations throughout West Hawaii. Low-level wells contained between 40%-93% “young” water whereas high-level wells had 5%-41% “young” water, demonstrating that it is possible to differentiate high-level water from basal aquifer water based on its chemical composition. It also indicates

that much of the water in the West Hawaii study area is a mixture of young and old water (Kelly and Glenn, 2015).

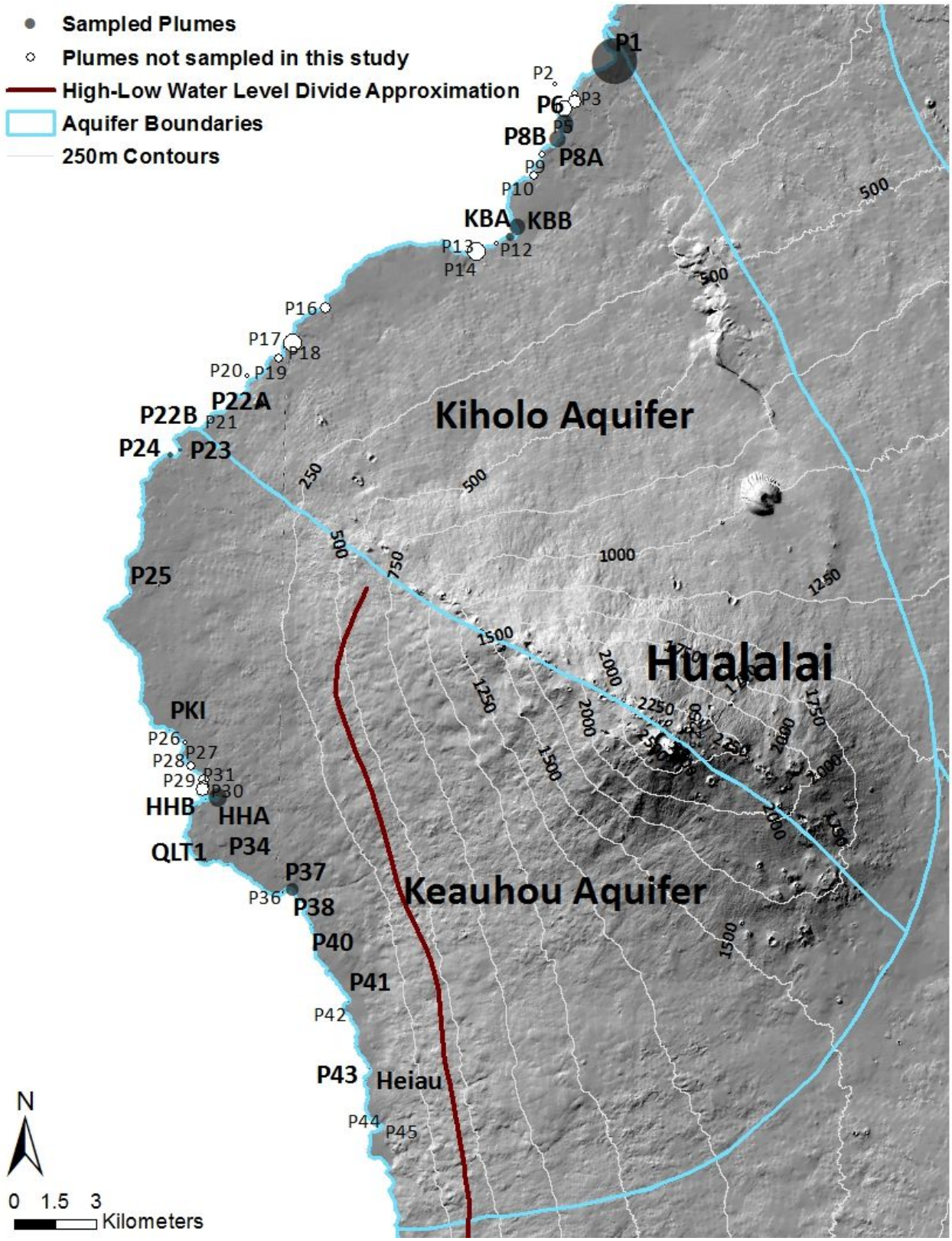

Figure 1.3 Map of the West Hawaii study area with the Keauhou and Kiholo aquifers. Black circles indicate locations of the sampled coastal springs. Open circles indicate springs identified in previous

studies (Johnson, 2008; Waters, 2015) not sampled in this project. Circle size is based on literature values for total SGD (m^3/d) (Table 1.2). The high water level—basal lens divide is shown. The divide is an approximation drawn based on known well head levels (Brytne Okuhata, personal communication, 2018).

Submarine Groundwater Discharge

In an island setting, freshwater exists as a lens that floats on top of denser seawater, and that mixing between the freshwater lens and seawater creates a brackish zone. Inputs to the freshwater lens originate as recharge in the form of precipitation, irrigation, fog drip, and waste water injection, among others. Outputs included pumping and SGD, as well as evapotranspiration. While each of these factors affects the amount of SGD discharging at any given time, over a period of years it averages out and becomes relatively steady-state. Over time, due to gravity and pressure from water entering the aquifer, the fresh groundwater is forced to discharge. The physical principles of Ghyben-Herzberg state that under ideal conditions, for every foot of fresh water above sea level, 40 feet of fresh water exist below sea level at any given location and that this lens thins out near the coast. It is known that at least part, if not all, of groundwater discharge occurs at the coastline and can often be identified by its colder temperature and lower salinity. It should be noted that at the point of discharge, the groundwater is usually no longer entirely fresh but has become brackish due to seawater intrusion, tidal forcing, wave setup, storm surge, and sea level fluctuation, or a combination of these factors (Knee et al., 2008; Dulai et al., 2015).

As stated above, groundwater begins its journey as freshwater precipitation at higher elevations and on its journey may mix with more brackish water from seawater intrusion into the mixing zone of the aquifer. Therefore, groundwater can usually be identified by its colder temperature (due to its origin in colder climates) and lower salinity. Another tracer of groundwater is the element radon. Radon is a naturally occurring gas that comes from the breakdown of uranium in soil, rock, or water (Oram, 2014). In the West Hawaii study area, radon leaches out of the basalt and into the groundwater that flows through it. This causes groundwater to be enriched in radon compared to seawater or surface water (Peterson et al., 2009). Because radon is significantly more concentrated in groundwater than surface water (usually 1000-fold or greater), it makes for an excellent tracer of SGD at the shoreline (Burnett and Dulaiova, 2003). Because of radon's unique association with groundwater, it can be used to measure the amount of groundwater discharge from the coastal aquifer (Burnett and Dulaiova, 2003; Peterson et al., 2009; Knee et al., 2010; Dudley et al., 2014; Waters, 2015).

In the Kona study area, SGD has been quantified at multiple locations along the coastline using a variety of techniques, including thermal infrared (TIR) imaging, salinity and silicate mass balance, and radon time-series and box models. For example, SGD fluxes in Kiholo Bay have been calculated and range from 2,300 m^3/d (Waters, 2015) to 25, 289 m^3/d (Johnson, 2008). Combined with other studies, the average SGD rate is 11,000 m^3/d (Johnson, 2008; Peterson et al., 2009; Dimova et al., 2012; and Waters, 2015). Honokohau Harbor has also been studied extensively and has a range of SGD rates from 5,500 m^3/d to 35,970 m^3/d with an average of 9,934 m^3/d (Oki, 1999; Johnson, 2008; Johnson et al., 2008; Peterson et al., 2009; Waters, 2015). For comparison, the only gauged stream in the area, Waiahu stream, has an annual mean discharge of 270 m^3/d (USGS Station 16759600).

Methods:

Sampling Sites

Coastal spring sampling sites were chosen based on previously identified SGD locations using TIR imaging by Johnson (2008). Waters (2014) identified SGD locations from radon surveys, as well as field surveillance where a conductivity meter was used to locate brackish water at the coastline. A total of 49 coastal discharge plumes along the coastline of the combined Kiholo and Keauhou aquifers were identified. Of the 49 sites identified, 24 were chosen to be sampled in this study based on accessibility and to achieve a relatively even sampling distribution within both aquifers. Although the general locations of the SGD plumes were known, the exact discharge points were located based on salinity measurements of the coastal water using a multiparameter probe (YSI V2-2 600XLM Sonde). Eight sites were sampled multiple times and led to a total of 49 samples (Figure 1.3).

Three sites, Kiholo Bay, Honokohau Harbor, and P1 (Anaehoomalu Bay), were chosen to have time-series measurements for radon, stable isotopes, and salinity performed. Kiholo and Honokohau were chosen for time-series sampling to check if discharge during our study matched discharge rates previously identified because these sites have both been extensively studied (Oki, 1999; Johnson, 2008; Johnson et al., 2008; Street et al., 2008; Peterson et al., 2009; Knee et al., 2010; Dimova et al., 2012; Waters, 2015; Dulai et al., 2016). P1 was chosen for the time-series measurement because the only known recorded SGD rate was an order of magnitude higher (78,089 m^3/d) than other spring discharge rates determined in the area (6,744±3,861 m^3/d) (Johnson, 2008). An independent, different approach, using in-situ radon

time series measurements and mass balance calculations, was used to derive SGD rate at this site.

Sampling Methods

Coastal groundwater samples were collected from 24 separate locations over four sampling efforts between November 2016 and August 2017. To prevent groundwater dilution with seawater, the sampling was done during low tide and the samples were collected using a stainless steel push-point sampler, which was inserted into the coastal substrate (rubble, sand, and rock crevices) 0.1-0.6 m deep. A peristaltic pump with silicone tubing was used to draw water into the sampling bottles. Before samples were collected, temperature, conductivity and dissolved oxygen were measured in the field using a multi-parameter sonde (YSI V2-2 model 600XML)

For water oxygen and hydrogen isotope samples, 60 mL acid-cleaned plastic bottles and caps were rinsed three times with sample water and then allowed to overflow for three bottle volumes before being filled. They were capped quickly to prevent evaporation, and no airspace was left in the bottle. The same methods were also performed when sampling for radon, though radon samples were collected and stored in 250 mL glass bottles.

For the radon time-series sampling, a RAD7 with a RAD-Aqua attachment was used (DURRIDGE Company, Inc.). Continuous sampling was performed for an entire tidal cycle at each of the three locations. Kiholo Bay and Honokohau Back Harbor were both sampled in November, 2016 while P1 was sampled in June, 2017. In the RAD-Aqua portable radon-in-air monitor, radon gas is extracted from the water and funneled into a closed recirculating air loop.

The instrument continuously measures the radon activity in that air loop (Lane-Smith et al., 2002; Schubert et al., 2003). Salinity and temperature data were collected concurrently using a conductivity, temperature, and depth recorder (Schlumberger CTD diver), which was attached to the head of the water pump and was used to correct for tidal fluctuations. Wind data was recorded at a nearby weather station (NWS Station PHKO).

Analytical Methods

Groundwater samples were analyzed for $\delta^{18}O$ and $\delta^{2}H$ values of water at the University of Hawai'i Stable Isotope Biogeochemistry Lab, Honolulu, HI using an L2130-i Picarro following the methods of Godoy et al., 2012. All samples were analyzed in at least triplicate and calibrated with NIST reference materials. Isotopic values were reported in δ-notation relative to Vienna Standard Mean Ocean Water (V-SMOW):

$$\delta^{18}O = \left(\frac{\left(\frac{\delta^{18}O}{\delta^{16}O}\right)_{sample}}{\left(\frac{\delta^{18}O}{\delta^{16}O}\right)_{standard}} - 1 \right) * 1000 \qquad (1)$$

Analytical uncertainty was determined by taking the average of the triplicate runs and calculating the standard deviation from the average for each sample.

Radon grab samples were analyzed using a RAD7 with a RAD-H_2O attachment that measures radon in air (DURRIDGE Company, Inc.). This instrument detects ^{218}Po, a decay product of the gaseous ^{222}Rn ($t_{1/2}$=3.82 days), which is degassed from the water sample into the detector chamber. Results are then decay-corrected with a half-life of ^{222}Rn to the time of sample collection.

SGD variability was determined using a radon mass-balance model (Dulai et al., 2015). This model accounts for radon inputs and outputs in the coastal zone over time. Radon is measured in the surface water, groundwater, offshore ocean, and atmosphere. The model accounts for coastal SGD plume thickness, radon (^{222}Rn) produced from its parent ^{226}Ra activity dissolved in the surface water, radon evasion to the atmosphere, and mixing losses. Changes in ^{222}Rn concentration over time are converted to radon fluxes due to SGD inputs (Burnett and Dulaiova, 2003). Using these parameters, SGD ($m^3/m/d$) can be calculated as total volumetric discharge (m^3/d) (Dulai et al., 2015).

Salinity Correction of Groundwater Samples

All samples were assumed to be a mixture of seawater intrusion into the aquifer and fresh meteoric water (assumed to have salinity of 0) (Waters, 2015; Fackrell, 2016). Ocean water end-member salinity and isotopic values were obtained from measurement of surface ocean water 1 km offshore from the Natural Energy Laboratory of Hawaii Authority facility collected in December 2016, which matched those reported by previous research (Fackrell, 2016). Using a two end-member mixing equation, ocean water end-member salinity values were used to correct the $\delta^{18}O$ and $\delta^{2}H$ isotopic values of groundwater samples for seawater content by mass balance (Scholl et al., 1996). The equation used was as follows:

$$\delta^{18}O_{\text{corrected}} = \frac{\delta^{18}O_{\text{sample}} - (\text{Sal}_{\text{ocean}} * \text{fraction}_{\text{sw}})}{\text{fraction}_{\text{fw}}} \quad (2)$$

where $\delta^{18}O_{\text{corrected}}$ is the $\delta^{18}O$ value corrected for ocean isotope contribution, $\delta^{18}O_{\text{sample}}$ is the value measured in a coastal spring of a given salinity, $\text{Sal}_{\text{ocean}}$ is the salinity of offshore seawater,

$fraction_{sw}$ is the fraction of seawater in the spring sample determined using salinity values, and $fraction_{fw}$ is the fraction of freshwater in the spring sample determined using salinity values, where $fraction_{sw}+fraction_{gw} = 1$. This approach assumes that the entirety of the saline component of SGD was recharged to the aquifer from recirculated surface seawater (Waters, 2015). Because we sampled nearshore SGD from the shallow part of the coastal aquifer, we did not have to consider seawater intrusion from the deeper layers of the ocean that have a slightly different isotopic signature (Fackrell, 2016). It also assumes that the oxygen isotopes of seawater evenly mixed with those of the freshwater component in proportion to the change in salinity. In addition, we assume that evaporation does not affect the signature of these isotopes during the mixing of ocean and groundwater in the subterranean estuary, which is a fair assumption because we used the push-point sampler to reach the groundwater before it discharged into the ocean and was subjected to evaporation.

Fresh Groundwater Discharge Estimates

In order to estimate the total amount of SGD in the Keauhou and Kiholo aquifers, literature values of available SGD estimates in the study area were compiled (Johnson, 2008; Street et al., 2008; Peterson et al., 2009; Knee et al., 2010; Dimova et al., 2012; Tillery and El-Kadi, 2012; Dulai et al., 2015; Waters, 2015). These studies used a variety of methods to calculate discharge rates, including thermal infrared imaging, radon time-series measurements followed by a radon mass balance model (Burnett and Dulaiova, 2003), a radium mass balance model (Street et al., 2008) and estimates based off of TIR-identified plume area or length of coastline containing the plume. All these estimates are snap-shot measurements representing

SGD averaged over a tidal cycle to avoid bias towards low or high tide values. Where multiple literature values are referenced for a single plume, the average of the values was calculated. Original plume site names and locations were based on the work of Johnson (2008), who performed the most inclusive study of the region.

Because of the difficulty in assessing the fresh component only of SGD, the majority of these studies only report total (a combination of fresh and saline) values of SGD, therefore fresh discharge was estimated by comparing the few reports containing values for both freshwater and brackish SGD. This method assumes that freshwater comprises the remainder of the total SGD after the recirculated seawater component was subtracted (Waters, 2015). Using this method and comparing it to salinity values measured in situ with the YSI sonde, it was determined that the majority of SGD in this area contains roughly 30-80% freshwater (Table 1.1 and 1.2).

Reconstruction of Coastal Spring Isotopic Signatures Using an Integrated Recharge Flow Path

In this study, $\delta^{18}O$ isotopes of recharge were calculated using one of two methods, depending on whether the elevation fell above or below the 2000m inversion boundary. If recharge occurred below 2000m, then Fackrell's (2016) equation was used:

$$\delta 18O = -0.0012(\mathrm{h}) - 3.27 \quad (3)$$

Whereas if recharge occurred above 2000m, Scholl et al.'s (1996) equation was used:

$$\delta 18O = -0.00319(\mathrm{h}) - 0.45 \quad (4)$$

where (h) is elevation in meters (Scholl et al., 1996; Fackrell, 2016). These two equations were used to solve for recharge $\delta^{18}O$ values at varying elevations (Scholl et al., 1996; Fackrell, 2016). These equations were created based on empirical data collected from rain collectors positioned in the West Hawaii study area and near the summits of Mauna Loa and Kilauea (Scholl et al., 1996; Fackrell, 2016). In these studies, it was assumed that the $\delta^{18}O$ of the groundwater at any given location represented an integration of the recharge along the groundwater's potential flow path upstream of that point and the fraction of contribution of each location to the isotopic signature is driven by the fraction of recharge at that location from the total recharge along the flow path. It was also assumed that these same trends held for elevations leading up to Mauna Kea, despite a lack of precipitation collectors in that area to confirm this.

Next, the salinity-corrected $\delta^{18}O$ from the coastal spring was compared to the calculated $\delta^{18}O$ of recharge at increasing distances upslope and along different flow paths:

$$\delta^{18}O_{sample} = \frac{\sum_{int=1}^{n} \delta^{18}O(n) * R(n)}{\sum_{int=1}^{n} R(n)} \qquad (5)$$

where $\delta^{18}O(n)$ is the isotopic value of precipitation for the interval *n*, which was calculated using equations 2 and 3 (Scholl et al., 1996; Fackrell, 2016). R(*n*) is the estimated recharge volume for the elevation interval *n* and was calculated from an existing USGS recharge map using ArcGIS (Engott, 2011; ESRI, 2016). In the original study performed by Engott (2011), mean annual groundwater recharge was estimated for the period 1984-2008 for the entire Island of Hawaii. The model accounted for fog interception, rainfall, irrigation, evapotranspiration, water stored in the root zone, wastewater injection, and runoff. All of these factors were taken into account to calculate groundwater recharge. Then, areas were grouped into regions of similar

groundwater recharge and assigned a recharge rate to each region in units of meters cubed per day to investigate different recharge rates along groundwater flow paths in West Hawaii (Engott, 2011).

Using intervals of 250m and inserting these elevation intervals into either equation (3) or (4) depending on the elevation of the current section of the assumed flow path, the integration began at the sampling site elevation (zero meters at all sites sampled) and proceeded upslope until the sample and integrated recharge $\delta^{18}O$ values were equivalent (Scholl et al., 1996; Fackrell, 2016). Intervals of 250 meters were chosen based on the resolution of the recharge coverage. Multiple flow path directions were plotted for each plume group and recharge was calculated for each potential integrated path. For some plume groups, multiple flow paths from different sources were needed to reach the coastal spring isotopic signature. This will be explained in further detail below.

This approach assumes that there is a steady rain-out effect as elevation increases, which does not account for the saddle region between Hualalai and both Mauna Kea and Mauna Loa, where no precipitation collectors were placed (Fackrell, 2016). In this region, the rain-out of heavier oxygen isotopes would still occur as the water vapor moves inland, but the elevation is decreasing for a short distance instead of consistently continuing to increase. Although this is an assumption we must make given the current studies performed in the area, more research is needed, particularly deploying rain collectors distributed throughout the higher regions of Mauna Kea and Mauna Loa.

Results:

Chemical Parameters of Groundwater

Salinities of the collected spring samples depended both on the salinity of the coastal aquifer groundwater and on tidal pumping at the time of sample collection. Although we aimed to collect samples at low tide, the samples were collected on multiple days with different low tide levels. The salinities reported here (Table 1.1) therefore do not necessarily reflect the salinity of the coastal aquifer only. At several locations samples were collected throughout a full tidal cycle. This can be seen at site KBA, where the salinities of the samples varied from 12.7-32.2 between low and high tides respectively, showing the significant effect tidal pumping exerts on coastal spring salinities.

Salinity-corrected groundwater $\delta^{18}O$ was averaged for sampling sites that had multiple samples. Including all individual sites, $\delta^{18}O$ values ranged from -1.26‰ to -9.16‰ (average -5.79‰) while $\delta^{2}H$ averaged values ranged from -9.58‰ to -62.34‰ (average -36.01‰). Standard deviations ranged from 0.01‰ to 2.12‰ (average 0.30‰) for $\delta^{18}O$ and 0.27‰ to 28.43‰ (average 4.68‰) for $\delta^{2}H$. It should be noted that samples at OKA and KBA with salinity 33 or higher collected at high tide were omitted in the average calculations because the salinity correction would introduce a large error, as those samples have little groundwater influence and long coastal residence time, and therefore experience greater fractionation due to evaporation.

Generally, heavier oxygen and hydrogen isotopes were more depleted in the Kiholo Aquifer and less depleted in the Keauhou Aquifer. These values are similar to those collected in 2008 and reported by Kelly and Glenn (2015) and values collected in 2011-2012 reported by Fackrell (2016) at nearby locations. For both aquifers, the hydrogen isotopes had greater

uncertainty, confirming our need to perform calculations that rely on the oxygen isotopes to ensure greater accuracy and reliability. Oxygen isotopes also have a more consistent relationship with elevation (Scholl et al., 1996; Scholl et al., 2002; Fackrell, 2016).

Salinity-corrected radon collected from springs was also averaged for sampling sites that had multiple samples. The entirety of the radon values ranged from 0 Bq/m^3 to 1370 Bq/m^3 (average 383 Bq/m^3). Standard deviations ranged from 4 Bq/m^3 to 2520 Bq/m^3 (average 586 Bq/m^3). Generally, Kiholo Aquifer had lower radon values and uncertainties, whereas Keauhou Aquifer trended toward higher radon values.

The presence of radon was apparent in all samples collected at low tide, indicating the presence of groundwater and confirming that we sampled SGD rather than surface runoff, the absence of which was also confirmed during site visits. The samples analyzed using the RAD-H2O had higher uncertainties because this method is less sensitive than the RAD-Aqua and the samples were analyzed with a few hours delay after collection. The uncertainty was significantly lower for the samples that were analyzed using the RAD-Aqua time-series method, which has better sensitivity and which measures radon immediately on-site.

Sample Name	Aquifer	Site Name	n	Salinity	$\delta^{18}O$‰	$\delta^{2}H$‰	Radon Bq/m^3
P1	Kiholo	Anaehoomalu Bay	4	6.45	-9.16±0.02	-62.34±0.47	54±264
P6	Kiholo	Pueo Bay	1	5.46	-8.69±0.01	-58.75±0.27	59±346
P8A	Kiholo	N. Keawaiki Bay	1	10.50	-7.94±0.08	-52.92±1.00	63±260
P8B	Kiholo	S. Keawaiki Bay	1	5.44	-8.68±0.02	-58.35±0.34	119±393
KBB	Kiholo	Kiholo Bay	4	23.27	-7.52±0.23	-51.91±3.79	NA
KBA	Kiholo	Kiholo Bay Inlet	7	23.10	-7.24±0.39	-48.58±5.89	745±15
P22A	Kiholo	N. Puu Alii Bay	1	NA	-3.89±0.17	-21.44±2.05	128±656
P22B	Kiholo	S. Puu Alii Bay	1	17.65	-5.05±0.14	-27.78±2.57	508±917
KIHOLO AQUIFER AVERAGE				**13.12**	**-7.08±0.13**	**-47.76±2.05**	**239±407**
P23	Keauhou	N. Mahaiula Bay	1	NA	-5.03±0.02	-26.33±0.34	414±696
P24	Keauhou	S. Mahaiula Bay	1	26.34	-5.48±0.30	-37.51±6.90	103±784
P25	Keauhou	Makako Bay	1	26.90	-5.45±0.64	-33.39±8.07	197±804
PK	Keauhou	Kohana Iki	2	15.59	-6.57±0.13	-39.57±2.01	181±581
HHA	Keauhou	Honokohau Back Harbor	6	21.16	-4.73±0.31	-30.10±6.13	2918±4
HHB	Keauhou	Honokohau Harbor Fuel Dock	4	26.73	-3.97±0.50	-24.99±8.48	NA
QLT1	Keauhou	Queen Liliuokalani Trust	1	32.22	-1.26±2.12	-14.40±28.43	374±748
P34	Keauhou	N. Old Kona Airport	1	23.72	-4.79±0.24	-24.86±4.77	228±927
OKA	Keauhou	S. Old Kona Airport	4	31.44	-3.44±1.36	-9.58±20.23	NA
P37	Keauhou	Kailua Bay Swimming Beach	1	26.84	-5.40±0.50	-31.00±8.07	1370±2520
P38	Keauhou	Kailua Bay	1	16.58	-3.99±0.16	-17.30±2.07	324±827
P39	Keauhou	Oneo Bay	1	11.74	-4.02±0.08	-15.73±1.22	688±932
P40	Keauhou	S. Holualoa Bay	1	12.80	-3.12±0.11	-15.97±1.37	173±536
P41	Keauhou	White Sands Beach	1	27.65	-4.13±0.63	-23.32±8.86	0±457
P43	Keauhou	Kahaluu Bay	1	16.77	-3.46±0.14	-18.27±2.27	148±761
Heiau	Keauhou	Heiau	3	5.20	-5.12±0.01	-26.59±0.39	255±138
KEAUHOU AQUIFER AVERAGE				**21.45**	**-4.50±0.46**	**-24.31±6.85**	**527±765**

Table 1.1 Groundwater characteristics of coastal springs. $\delta^{18}O$, $\delta^{2}H$, and radon values are corrected for salinity. For raw data, see Appendix Table A.1. Samples are ordered from north to south and are divided by aquifer boundaries.

Literature Rates for Submarine Groundwater Discharge, Recharge, and Pumping for West Hawaii

Submarine groundwater discharge fluxes calculated in previous studies found that fresh SGD fluxes were higher in Kiholo Aquifer than in Keauhou Aquifer (Table 1.2). This may in part be due to an incomplete dataset within Keauhou Aquifer, where a few known locations of springs have not had SGD fluxes measured (P40-P45). Therefore, the total flux of the Keauhou Aquifer should be considered an underestimate of the true value.

Although the SGD fluxes are higher for Kiholo, there is a lower recharge rate than that of Keauhou, with the difference between the recharge rates of the two aquifers being 243,638 m^3/d. The areas of Kiholo Aquifer and Keauhou Aquifer are comparable: 381 km^2 and 425 km^2, respectively. The recharge rates were calculated only for the area contained within the aquifer boundaries as denoted by Engott (2011) and do not include recharge rates or groundwater inflow from aquifers that are further upslope of the two aquifers that comprise the study area.

For the West Hawaii study area, pumping is greater in Keauhou Aquifer (55,167 m^3/d) than it is in Kiholo Aquifer (34,010 m^3/d) (Commission On Water Resources Management, unpublished data, 2017). This likely stems from the higher concentration of people and urbanized land cover that occurs in Keauhou Aquifer as opposed to the mostly barren rock or scrubland found in Kiholo Aquifer.

Table 1.2 Table depicting submarine groundwater discharge rates along the Kona coast. In cases of multiple samples from one site, values were taken from the sample exhibiting the lowest salinity. Where multiple literature values are referenced, the average of the values was calculated and reported. Original spring site names and locations taken from Johnson, 2008. Fresh SGD was calculated using measured salinity where available and assuming a 60% freshwater component where salinity measurements were unavailable. Stars indicate time-series SGD locations.

Sampled Springs	All Springs	Aquifer	Site Name	Latitude	Longitude	Salinity	Fresh SGD (%)	Total SGD (m^3/d)	Fresh SGD (m^3/d)	Recharge (m^3/d)	Pumping (m^3/d)	References
★ P1	P1	Kiholo	Anaehoomalu Bay	19.9139	-155.8876	5.17	85	78,089	66,376			Johnson, 2008
	P2	Kiholo	South of Anaehoomalu Bay	19.9058	-155.9083	NA		2,300	1,380			Johnson, 2008
	P3	Kiholo	N. Akahu Kaimu	19.9031	-155.9011	NA		2,959	1,775			Johnson, 2008
	P4	Kiholo	S. Akahu Kaimu	19.9003	-155.9011	NA		6,779	4,067			Johnson, 2008
	P5	Kiholo	Weliweli	19.8978	-155.9047	NA		7,000	4,200			Johnson, 2008
P6	P6	Kiholo	Pueo Bay	19.8931	-155.9047	5.46	84	12,239	10,281			Johnson, 2008
P8A	P7	Kiholo	N. Keawaiki Bay	19.8880	-155.9067	10.50	70	11,289	7,902			Johnson, 2008
P8B	P8	Kiholo	S. Keawaiki Bay	19.8867	-155.9070	5.44	84	4,639	3,897			Johnson, 2008
	P9	Kiholo	Kaiwi Pt.	19.8828	-155.9125	NA		3,000	1,800			Johnson, 2008
	P10	Kiholo	Ohiki Bay	19.8758	-155.9150	NA		3,500	2,100			Johnson, 2008
KBB	P11	Kiholo	Kiholo Bay	19.8586	-155.9206	15.46	57	11,000	8,800			Johnson, 2008; Peterson et al., 2009; Dimova et al., 2012; Waters, 2015
★ KBA	P11	Kiholo	Kiholo Bay Inlet	19.8554	-155.9229	12.70	81	11,000	8,910			Johnson, 2008
	P12	Kiholo	Mid-N Kiholo Bay	19.8531	-155.9278	NA		1,689	1,013			Johnson, 2008
	P13	Kiholo	Mid-S Kiholo Bay	19.8506	-155.9344	NA		329	197			Johnson, 2008
	P14	Kiholo	S Kiholo Bay	19.8503	-155.9344	NA		8,289	4,973			Johnson, 2008
	P15	Kiholo	SS Kiholo Bay	19.8494	-155.9386	NA		6,419	3,851			Johnson, 2008
	P16	Kiholo	Kahuwai Bay	19.8311	-155.9869	NA		5,589	3,353			Johnson, 2008
	P17	Kiholo	Kukio Bay	19.8192	-155.9981	NA		9,089	5,453			Johnson, 2008
	P18	Kiholo	Kikaua Pt	19.8178	-156.0008	NA		859	515			Johnson, 2008
	P19	Kiholo	Kakapa Bay	19.8142	-156.0028	NA		4,500	2,700			Johnson, 2008
	P20	Kiholo	Kua to Kahoiawa Bay	19.8083	-156.0136	NA		2,500	1,500			Johnson, 2008
	P21	Kiholo	Awakee Bay	19.7958	-156.0222	NA		559	335			Johnson, 2008
P22A	P22	Kiholo	N. Puu Alii Bay	19.7935	-156.0259	NA	54	1,559	842			Johnson, 2008
P22B	P22	Kiholo	S. Puu Alii Bay	19.7927	-156.0270	17.65	50	1,559	780			Johnson, 2008
KIHOLO AQUIFER TOTAL								**196,734**	**147,003**	**92,347**	**34,010**	Fukunaga, 2010; Engott, 2011; Tillery and El-Kadi, 2012

Sampled Springs	All Springs	Aquifer	Site Name	Latitude	Longitude	Salinity	Fresh SGD (%)	Total SGD (m^3/d)	Fresh SGD (m^3/d)	Recharge (m^3/d)	Pumping (m^3/d)	References
P23	P23	Keauhou	N. Mahaiula Bay	19.7833	-156.0365	NA	86	2,489	2,141			Johnson, 2008
P24	P24	Keauhou	S. Mahaiula Bay	19.7817	-156.0396	26.34	25	8,259	2,065			Johnson, 2008
P25	P25	Keauhou	Makako Bay	19.7356	-156.0530	26.90	23	689	158			Johnson, 2008
PKI	N/A	Keauhou	Kohana Iki	19.6913	-156.0382	15.06	57	Unknown	Unknown			
	P26	Keauhou	Kaloko Pond	19.6869	-156.0331	NA		2,089	1,253			Johnson, 2008; Knee et al., 2010
	P27	Keauhou	N. Kaloko Pt. ("The Cut")	19.6858	-156.0336	NA		369	221			Johnson, 2008
	P28	Keauhou	Kaloko Pt.	19.6794	-156.0308	NA		4,189	2,513			Johnson, 2008
	P29	Keauhou	Aimakapa Pond	19.6747	-156.0264	NA		4,900	2,940			Johnson, 2008; Knee et al., 2010
	P30	Keauhou	N. of Aiopio Fishtrap	19.6731	-156.0264	NA		5,300	3,180			Johnson, 2008
	P31	Keauhou	Aipio Fishtrap	19.6717	-156.0264	NA		6,029	3,617			Johnson, 2008
★ HHA	P32	Keauhou	Honokohau Back Harbor	19.6693	-156.0211	16.82	27	9,934	2,682			Oki, 1999; Johnson, 2008; Johnson et al., 2008; Peterson et al., 2009; Waters, 2015
HHB	N/A	Keauhou	Honokohau Harbor Fuel Dock	19.6685	-156.0255	22.85	28	Unknown	Unknown			
	P33	Keauhou	Noio Pt.	19.6631	-156.03111	NA		489	293			Johnson, 2008
QLT1	N/A	Keauhou	Queen Liliuokalani Trust	19.6489	-156.0212	32.22	8	Unknown	Unknown			
P34	P34	Keauhou	N. Old Kona Airport	19.6472	-156.0170	23.72	32	1,049	336			Johnson, 2008
OKA	P35	Keauhou	S. Old Kona Airport	19.6428	-156.0097	31.20	10	1,189	119			Johnson, 2008
	P36	Keauhou	Kailua Bay: Narrow Inlet	19.6383	-155.9978	NA		879	527			Johnson, 2008
P37	P37	Keauhou	Kailua Bay Swimming Beach	19.6389	-155.9976	26.84	23	529	122			Johnson, 2008
P38	P38	Keauhou	Kailua Bay	19.6397	-155.9948	16.58	53	8,989	4,764			Johnson, 2008; Knee et al., 2010
P39	P39	Keauhou	Oneo Bay	19.6354	-155.9907	11.74	67	549	368			Johnson, 2008
P40	P40	Keauhou	S. Holualoa Bay	19.6282	-155.9881	12.80	64	Unknown	Unknown			Johnson, 2008
P41	P41	Keauhou	White Sands Beach	19.6029	-155.9746	27.65	21	Unknown	Unknown			Johnson, 2008
	P42	Keauhou	White Sands Beach	19.5983	-155.9744	NA		Unknown	Unknown			Johnson, 2008
P43	P43	Keauhou	Kahaluu Bay	19.5811	-155.9668	16.77	52	Unknown	Unknown			Johnson, 2008
Heiau	N/A	Keauhou	Heiau	19.5770	-155.9680	4.43	87	Unknown	Unknown			
	P44	Keauhou	Keauhou Bay	19.5619	-155.9619	NA		Unknown	Unknown			Johnson, 2008
	P45	Keauhou	Maihi to Paaoao Bay	19.5619	-155.9619	NA		Unknown	Unknown			Johnson, 2008
KEAUHOU AQUIFER TOTAL								**57,920**	**27,301**	**335,985**	**55,167**	Fukunaga, 2010; Engott, 2011; Tillery and El-Kadi, 2012

Literature SGD and Sampled SGD Comparison

Tidally averaged SGD from our time-series measurements were in general agreement with rates reported by the literature at all three locations (Table 1.3). In the case of plume P1, our value (30,700 m^3/d) was significantly less than the value reported by Johnson (2008) (78,089 m^3/d). As for Kiholo Bay and Honokohou Harbor, our SGD rates (6,000 m^3/d and 12,500 m^3/d, respectively) are similar to those reported by others and fall within the range of values calculated in previous studies (Oki, 1999; Johnson, 2008; Johnson et al., 2008; Peterson et al., 2009; Dimova et al., 2012; Waters, 2015, Dulai et al., 2016).

Sampled Plumes	Aquifer	Site Name	Latitude	Longitude	Literature SGD (m^3/d)	Fresh SGD (m^3/d)	Sampled SGD (m^3/d)	Reference
P1	Kiholo	Anaehoomalu Bay	19.9139	-155.8876	**78,089**	**66,376**	**30,700**	Johnson, 2008
Kiholo Bay	Kiholo	Kiholo Bay	19.8554	-155.9229	25,289			Johnson, 2008
Kiholo Bay					7,100			Peterson et al., 2009
Kiholo Bay					9,200			Dimova et al., 2012
Kiholo Bay					2,400			Water, 2015
Kiholo Bay					5,700			Dulai et al., 2016
AVERAGE KIHOLO BAY					**9,938**	**8,800**	**6,000**	
Honokohau Harbor	Keauhou	Honokohau Back Harbor	19.6693	-156.0211	4,480			Oki, 1999
Honokohau Harbor					9,589			Johnson, 2008
Honokohau Harbor					12,000			Johnson et al., 2008
Honokohau Harbor					12,000			Peterson et al., 2009
Honokohau Harbor					11,600			Waters, 2015
AVERAGE HONOKOHAU HARBOR					**9,934**	**2,682**	**12,500**	

Table 1.3 Comparison of SGD values reported in previous studies with the values we obtained using the RAD-Aqua (DURRIGE Company, Inc.) measurements over a tidal period and a radon mass balance approach (Burnett and Dulaiova, 2003).

Discussion:

Comparison of Literature SGD and Measured SGD

At all three sites the time-series measurements resulted in SGD rates lower than those reported in the literature. In the case of plume P1, the site was chosen specifically because the reported SGD was an order of magnitude higher than other discharges in the area. The radon time series measurements only captured nearshore discharge but the thermal imagery suggests more groundwater flow ~0.5 km from the shore. This was not captured in our measurement. More SGD measurements should be taken at this site to confirm the total SGD for this area. For Kiholo Bay, SGD measured in this study falls in the same range as previously reported fluxes, especially considering the SGD variability over time reported for Kiholo Bay by Dulai et al. (2015).

SGD Isotopic Signature Comparison with the Local Meteoric Water Line

A local meteoric water line (LMWL) describes the relationship between δ^2H and $\delta^{18}O$ values of precipitation for a particular region and elevation. This relationship is defined by the Rayleigh fractionation of water isotopes that occurs during evaporation, condensation, and precipitation of water. The depletion of δ^2H and $\delta^{18}O$ of precipitation as water vapor moves inland and upslope follows a pattern that can be measured. In West Hawaii, the steep slopes result in consistent patterns of δ^2H and $\delta^{18}O$ depletion in precipitation that allows the use of these isotopes as reliable tracers of rainfall and therefore groundwater recharge elevations (Scholl, 1996; Fackrell, 2016). A previous study performed by Fackrell (2016) determined that the LMWL for the region encompassing West Hawaii can be calculated using the following equation:

$$\delta^2H=(7.65*\delta^{18}O)+15.25 \quad r^2=0.98 \qquad (6)$$

This equation was created using data taken from a total of 8 precipitation collectors scattered throughout the West Hawaii study area over a two-year sampling period. These were integrated rainfall samples as oppose to individual rain events (Fackrell, 2016). Groundwater sample δ^2H and $\delta^{18}O$ values from this study were plotted against the LMWL (Figure 1.4).

Similar to Fackrell's (2016) data, the SGD data plot to the right of the LMWL. This indicates a slight enrichment of groundwater $\delta^{18}O$ isotopes. The reason for this deviation could stem from isotopic fractionation during evapotranspiration or infiltration before the groundwater reaches the aquifer. It could also stem from deviations in the δ^2H and $\delta^{18}O$ values of precipitation during Fackrell's two-year collection period versus our sampling period (Fackrell, 2016). Another possible reason the sampled isotopes may be more depleted could be due to oxygen isotopic exchange between the groundwater and the surrounding rock at temperatures greater that 150°C. If this occurs, it would leave the groundwater more depleted in $\delta^{18}O$, but would not affect the δ^2H values, which can be observed in the data (McMurtry et al., 1977). As has been described by Johnson et al. (2008) groundwater flow in the Hualalai region preserves its cold signature after recharge and temperatures of SGD remain <30 ^oC, so it seems unlikely isotopic exchange affects groundwater in this region due to the high temperature threshold it needs to occur, though it is difficult to say for certain (Gary McMurtry, personal communication, 2018). Even acknowledging these differences, the similarities between the LMWL and the δ^2H and $\delta^{18}O$ values from groundwater samples, as seen by the error bars that overlap the LMWL, justify using the $\delta^{18}O$-elevation relationship as a method for determining aquifer recharge elevations and potential flow paths (Fackrell, 2016).

It should be noted that two samples taken from spring "OKA" and two samples taken from spring "KBA" contained salinity outliers identified using Grubb's outlier test and a one-sample *t*-test, and were therefore excluded from the discussion (Figure 1.4). Because we suspect these samples were subject to evaporation it was determined that the values for sample "OKA" would not be included in the discussion.

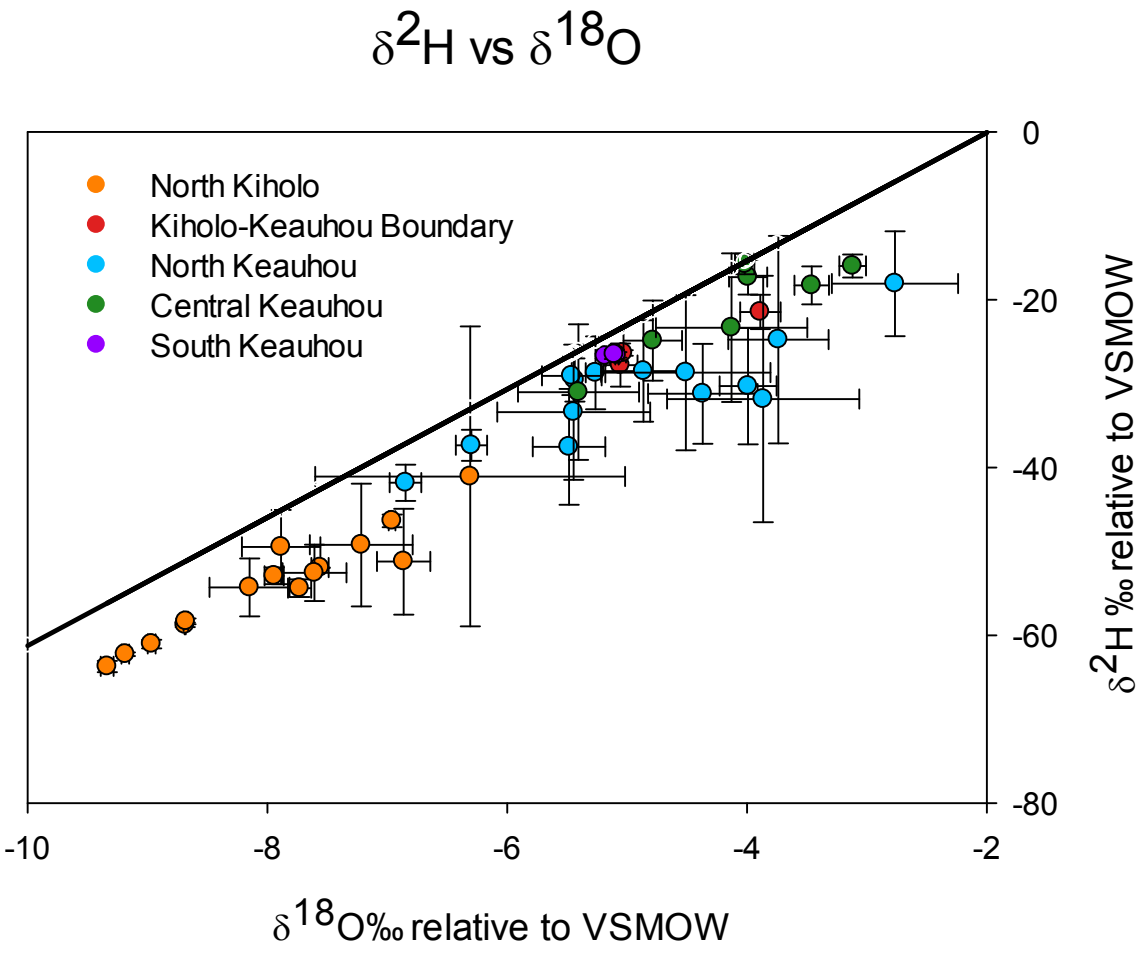

Figure 1.4. δ^2H vs $\delta^{18}O$ values plotted along with the West Hawaii LMWL with outlier OKA and KBA high-salinity values not included (Fackrell, 2016). Color reflects similarities of isotopic signatures of adjacent samples as defined in Table. 1.4.

SGD Isotopic Signatures

The $\delta^{18}O$ and $\delta^{2}H$ values of SGD showed that multiple samples from the same geographic regions showed similar isotopic signatures suggesting similar recharge origin. SGD locations were therefore grouped to reflect that groundwater feeding these SGD springs and outflows takes similar flow paths (Table 1.4). The distribution and extent of these groups is illustrated on Figure 1.5 with different groups assigned a different color for easy identification. The standard deviations of the average isotopic values in these groups show the largest variation of $\delta^{18}O$ and $\delta^{2}H$ values in the north and central Keauhou groups (blue and green). This is consistent with findings of Fackrell (2016) who suggested that there is large spatial heterogeneity in leakage from high level to basal aquifer in those regions.

Sample Name	Aquifer	Latitude	Longitude	n	Salinity	$\delta^{18}O$‰	$\delta^{2}H$‰
P1	Kiholo	19.91392	-155.88759	3	6.45	-9.16±0.02	-62.34±0.47
P6	Kiholo	19.89309	-155.90469	1	5.46	-8.69±0.01	-58.75±0.27
P8A	Kiholo	19.88796	-155.90671	1	10.50	-7.94±0.08	-52.92±1.00
P8B	Kiholo	19.88668	-155.90701	1	5.44	-8.68±0.02	-58.35±0.34
KBB	Kiholo	19.85855	-155.92062	4	15.46	-7.73±0.10	-54.39±1.04
KBA	Kiholo	19.85544	-155.92295	7	12.70	-7.56±0.07	-51.95±0.03
NORTH KIHOLO (ORANGE) GROUP AVERAGE					**9.34**	**-8.29±0.05**	**-56.45±0.53**
P22A	Kiholo	19.79354	-156.02589	1	NA	-3.89±0.17	-21.44±2.05
P22B	Kiholo	19.79274	-156.02695	1	17.65	-5.05±0.14	-27.78±2.57
P23	Keauhou	19.78330	-156.03651	1	NA	-5.03±0.02	-26.33±0.34
KIHOLO-KEAUHOU BOUNDARY (RED) GROUP AVERAGE					**17.65**	**-4.65±0.11**	**-28.27±2.97**
P24	Keauhou	19.78172	-156.03958	1	26.34	-5.48±0.30	-37.51±6.90
P25	Keauhou	19.73564	-156.05302	1	26.90	-5.45±0.64	-33.39±8.07
PK	Keauhou	19.69132	-156.03821	2	15.59	-6.57±0.13	-39.57±2.01
HHA	Keauhou	19.66926	-156.02108	6	16.82	-4.37±0.46	-31.19±5.96
HHB	Keauhou	19.66853	-156.02547	4	26.73	-4.86±0.35	-28.49±6.05
NORTH KEAUHOU (BLUE) GROUP AVERAGE					**22.48**	**-5.35±0.38**	**-33.16±5.52**
QLT1	Keauhou	19.64887	-156.02121	1	32.22	-1.26±2.12	-14.40±28.43
P34	Keauhou	19.64724	-156.01704	1	23.72	-4.79±0.24	-24.86±4.77
P37	Keauhou	19.63891	-155.99757	1	26.84	-5.40±0.50	-31.00±8.07
P38	Keauhou	19.63968	-155.99477	1	16.58	-3.99±0.16	-17.30±2.07
P39	Keauhou	19.63543	-155.99068	1	11.74	-4.02±0.08	-15.73±1.22
P40	Keauhou	19.62815	-155.98805	1	12.80	-3.12±0.11	-15.97±1.37
P41	Keauhou	19.60286	-155.97458	1	27.65	-4.13±0.63	-23.32±8.86
P43	Keauhou	19.58107	-155.96680	1	16.77	-3.46±0.14	-18.27±2.27
CENTRAL KEAUHOUA (GREEN) GROUP AVERAGE					**21.04**	**-3.77±0.50**	**-20.11±7.13**
Heiau	Keauhou	19.57699	-155.96798	3	5.20	-5.12±0.01	-26.59±0.39
SOUTH KEAUHOU (PURPLE) GROUP AVERAGE					**5.20**	**-5.12±0.01**	**-26.59±0.39**

Table 1.4 Salinity corrected groundwater $\delta^{18}O$ and $\delta^{2}H$ values. Samples are listed from north to south and are grouped by assumed similar recharge origin and groundwater flow path based on the similarity

of their $\delta^{18}O$ and $\delta^{2}H$ values. For locations where samples were collected during a full tidal cycle, the lowest salinity (representing low tide and therefore more groundwater) values were used.

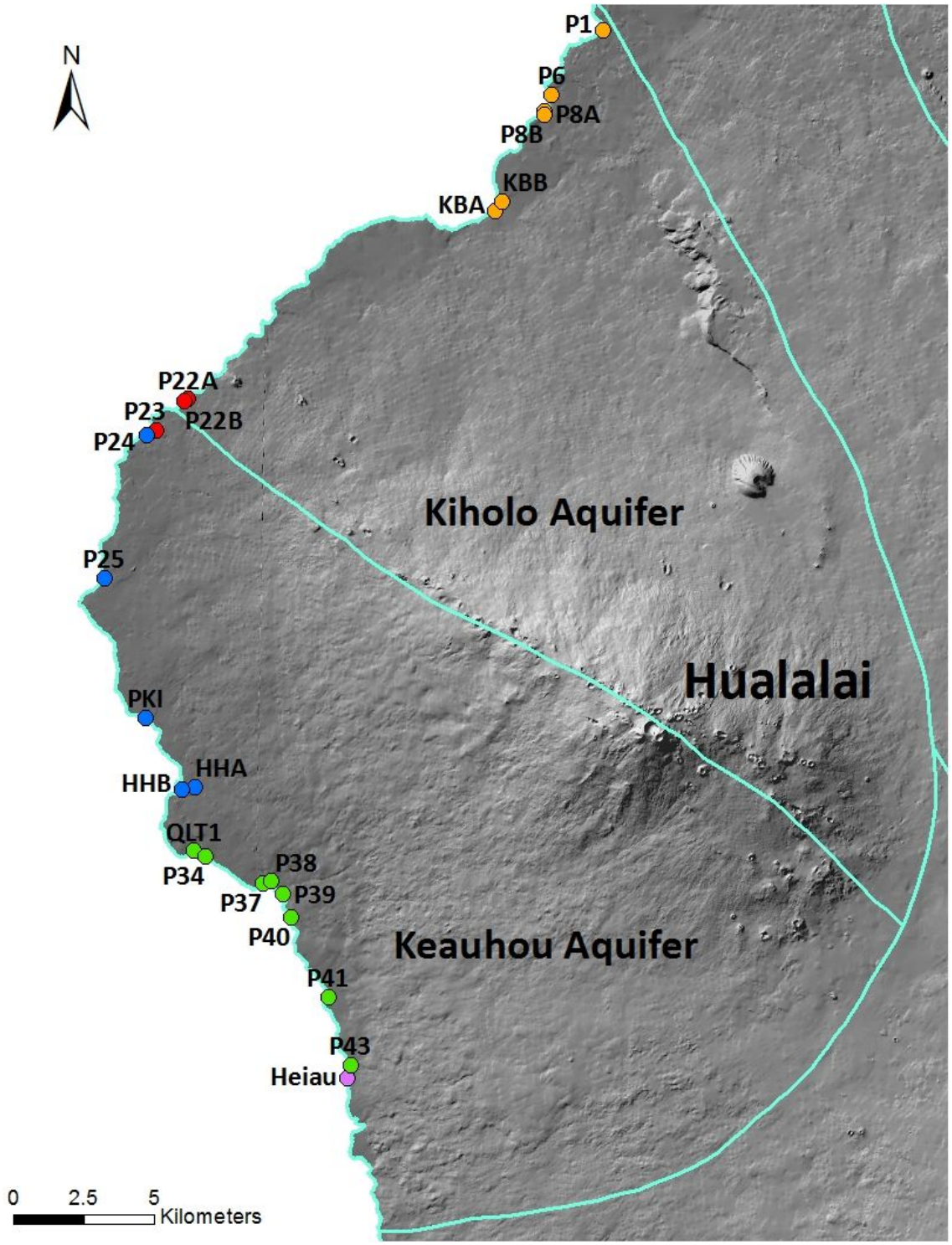

Figure 1.5. Map of the Kona study area showing SGD outflows grouped by assumed similar recharge origin and

groundwater flow path based on the similarity of their $\delta^{18}O$ and $\delta^{2}H$ values. Colors are defined in Table 1.4.

Groundwater Recharge Elevation and Possible Flow Path Scenarios

The isotopic signature of the coastal groundwater is an integrated signature that the water acquires as precipitation originating at different elevations infiltrates to the aquifer along groundwater flow paths. For each group of SGD outflows, flow paths were backtracked to reconstruct their isotopic signature while assuming that water would flow from high elevation toward the coast. The elevation target was chosen based on the target integrated isotopic signature measured in SGD.

Integrated recharge flow paths were calculated leading from each group of SGD outflows either as separate lines heading upslope to Hualalai, Mauna Kea, Mauna Loa, or a combination of recharge from the three (Figure 1.6). Note that the SGD collected at the coastline most likely represents a combined flow signature from multiple pathways. Previous research provided regressions between precipitation elevation and volume-weighted $\delta^{18}O$ of precipitation (Equation 5) and determined likely aggregate recharge altitudes using the isotopic signature of the freshwater samples (Scholl et al., 1996; Tillman et al., 2014; Fackrell, 2016). Calculations using Equation 5 were performed until either the aggregated $\delta^{18}O$ matched each group's sample $\delta^{18}O$, or the top of the individual volcanoes was reached, whichever came first (Figure 1.7).

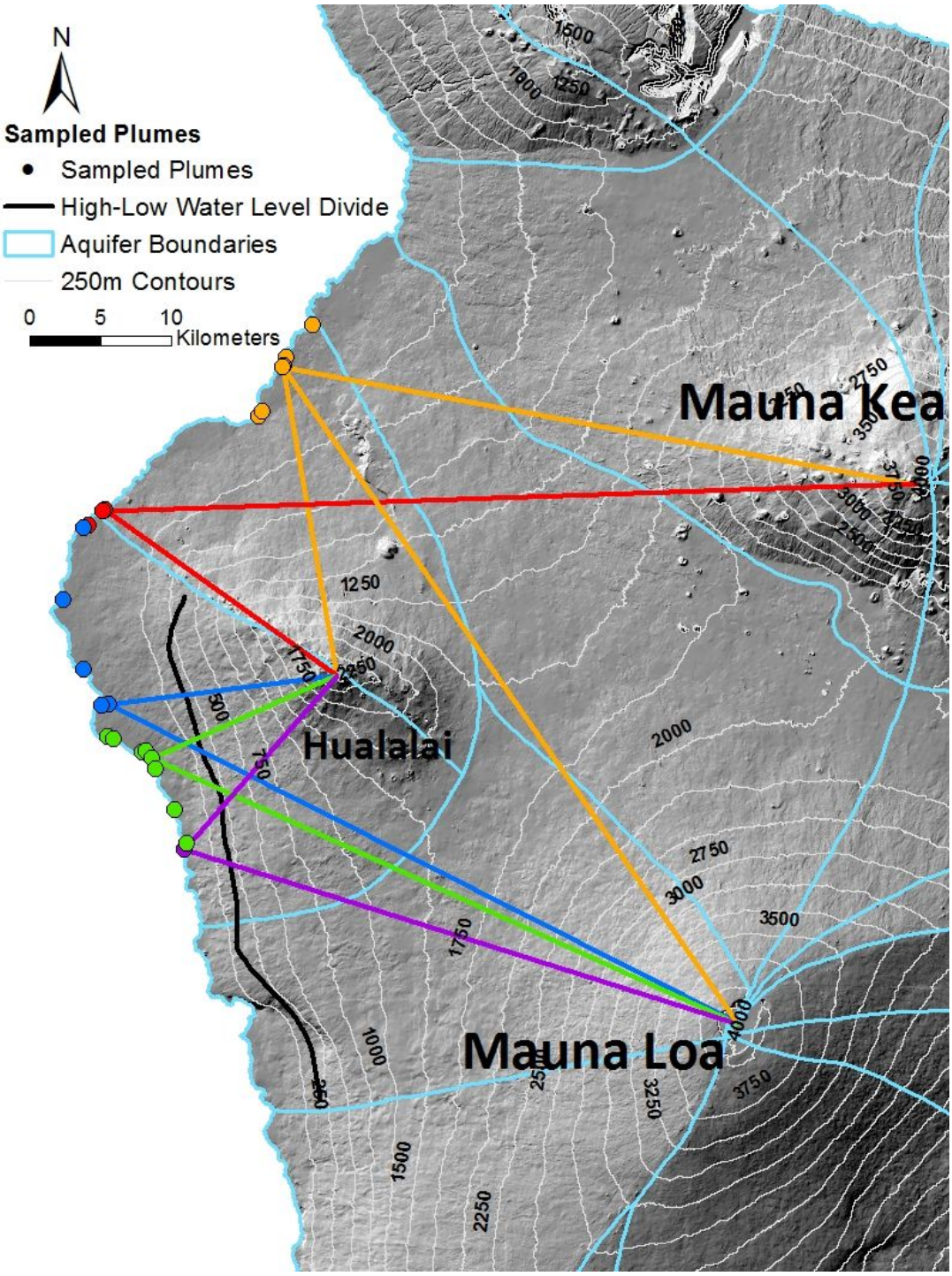

Figure 1.6. Map of the Kona study area showing potential recharge pathways leading from each of the grouped plumes upslope to the major three volcanoes.

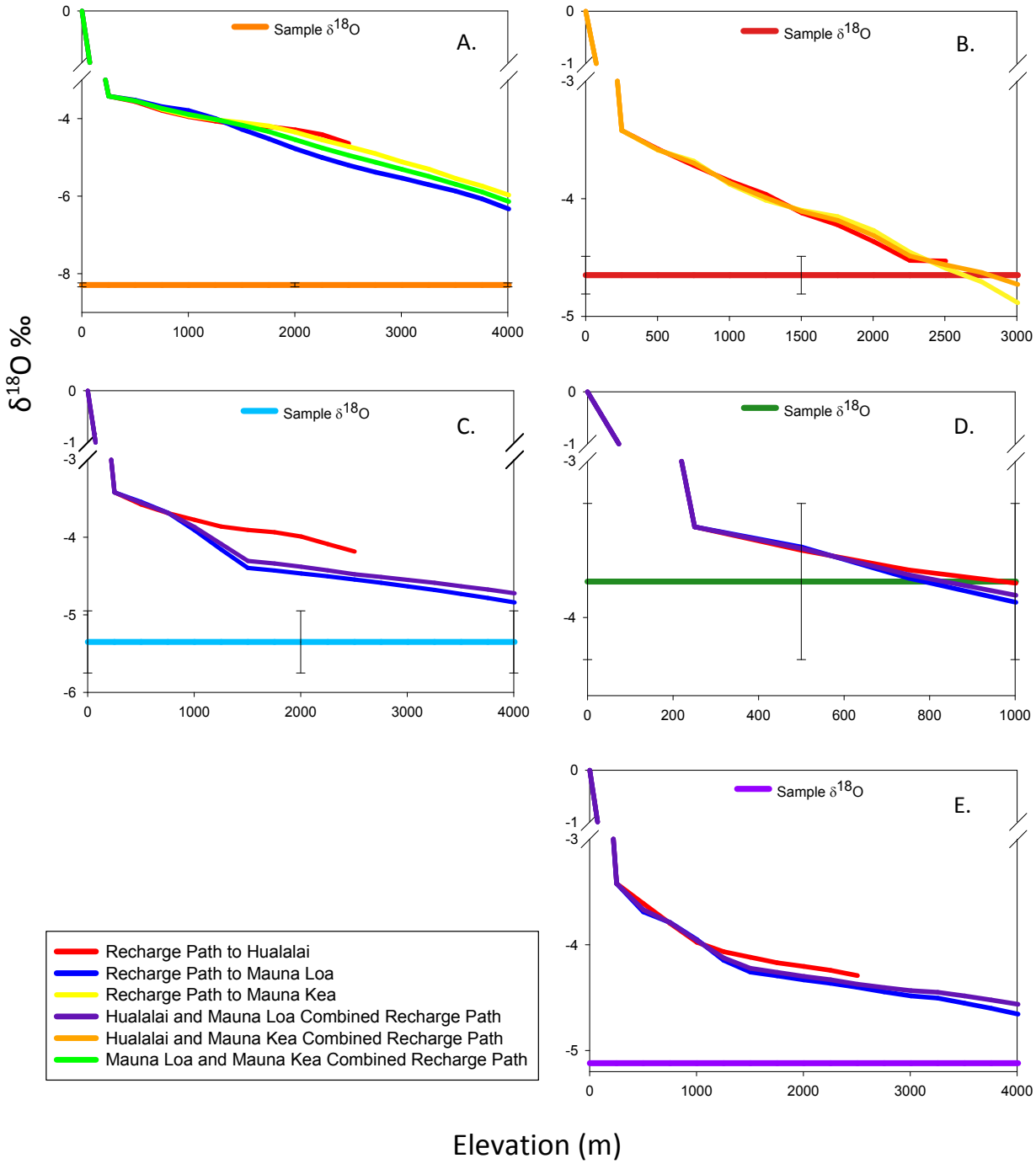

Figure 1.7 Potential recharge pathways leading from each of the grouped plume regions upslope to the main volcanoes. These pathways are shown on the map in Figure 1.6.

A. Represents recharge paths leading upslope from the North Kiholo Group.
B. Represents recharge paths leading upslope from the Kiholo-Keauhou Boundary Group.
C. Represents recharge paths leading upslope from the North Keauhou Group.
D. Represents recharge paths leading upslope from the Central Keauhou Group.
E. Represents recharge paths leading upslope from the South Keauhou Group.

North Kiholo Group

For the North Kiholo Group, none of the individual recharge paths matched the sample $\delta^{18}O$, despite carrying out Equation 5 to the tops of the volcanoes. Therefore, in order to account for the highly negative $\delta^{18}O$ values measured in SGD, it was determined that there must be another area contributing indirect recharge with a more depleted $\delta^{18}O$ than precipitation along the assumed recharge paths.

One possible area that may contribute indirect recharge was characterized by Adams et al. (1971), who used hydrogeophysical surveys using remote sensing to map out major structural features in West Hawaii. They speculate that a rift zone from the top of Hualalai leads down its northern slope and would divert groundwater to the north of Anaehoomalu Bay (the northernmost part of our West Hawaii study area). This is where an order of magnitude larger SGD was observed in comparison to other areas in the watershed. It also seems likely that the area downslope of this structure likely provides recharge to the coastline in Kiholo as well. A separate structure was inferred to lead down from Mauna Kea toward to coastline of Kiholo aquifer, suggesting that groundwater may be funneled from Mauna Kea to the coastline in this region (Adams et al., 1971).

It is also known that there is a deeper regional aquifer beneath the Humuula Saddle between Mauna Kea and Mauna Loa. This aquifer has a known highly-depleted groundwater $\delta^{18}O$ value of -10.4‰, believed to be so depleted because it is significantly older (on the timescale of roughly 7,000 years) (Donald Thomas, Hawaii Groundwater and Geothermal Resources Center, personal communication, 2018). Assuming that this upslope aquifer contributes more depleted $\delta^{18}O$ to Kiholo Aquifer than what is accounted for by the calculated

recharge rates, we calculated the amount of indirect recharge necessary to reach the sample $\delta^{18}O$ isotopic value using a two-end-member mixing line (Fackrell, 2016). We used -10.4‰ as one end-member, with the integrated recharge $\delta^{18}O$ value (-4.64‰) derived from contribution from both Mauna Kea and Mauna Loa recharge, as the other endmember. Assuming that there is a recharge contribution from either Mauna Kea (as suggested above based on findings by Adams et al. (1971)) or Mauna Loa or both, the indirect recharge from the saddle region would then account for 63% of the total recharge to the North Kiholo Group (Figure 1.8). This agrees with the results presented by Fackrell (2016) for samples taken from coastal wells and ponds in the same area.

Based on the work of Fackrell (2016), it seems less likely that this area would gain the entirety of its recharge from Hualalai. This hypothesis is further supported when using the North Kiholo Group sample $\delta^{18}O$ values into Equation 4. This equation, based on the isotopic precipitation at different elevations, predicts that water in these samples originates from elevations above 2,500m (the top of Hualalai). The predicted elevation is also above the upper fog belt boundary (2255m), indicating little influence from fog drip (Kelly and Glenn, 2015). Therefore, it appears the indirect recharge contribution from the saddle region accounts for the difference between the sample $\delta^{18}O$ and integrated $\delta^{18}O$ values, though there may also be some influence from Mauna Kea and Mauna Loa. This also agrees with the hypothesis that the aquifers are connected, with evidence of an upstream aquifer located beneath Humuula Saddle that contributes groundwater to coastal SGD.

Kiholo-Keauhou Boundary Group

For the Kiholo-Keauhou Boundary Group, based on watershed boundaries, it had been assumed that the entirety of the recharge originated from the slopes of Hualalai Mountain. The calculated integrated recharge flow path suggests that recharge on Hualalai alone can account for the $\delta^{18}O$ values measured in SGD, especially when sample $\delta^{18}O$ uncertainties are taken into account. Although a recharge path leading up to Mauna Kea was also calculated, this path seems unlikely to exist due to the long distance and indirect path relative to topographic contour lines.

Even though the exact groundwater flow paths for SGD springs in this group are unknown, it is noteworthy that the group spreads across the aquifer boundary and the northernmost part of Keauhou and southernmost part of Kiholo aquifers have the same groundwater flow paths. Current aquifer boundaries are based on surface topography and do not take into account subsurface geologic features, which may direct groundwater in a direction other than directly downslope. The data from the Kiholo-Keauhou Boundary group imply that the subsurface geology directs groundwater in a direction that does not always agree with surface topography, and that therefore the aquifer boundaries as we know them may not match subsurface flow.

North Keauhou Group

The North Keauhou Group SGD $\delta^{18}O$ and integrated $\delta^{18}O$ values were expected to match on a path that lead upslope to Hualalai's summit, yet the two values do not match for any of the tested recharge flow pathways (Figure 1.7). For these samples, it was determined that indirect recharge contributed isotopically light water to the coastal aquifer. Yet unlike the indirect recharge that contributes to the North Kiholo Group, the indirect recharge for the

North Keauhou Group does not seem to originate from the Humuula Saddle. In the Keauhou Aquifer, the high-level aquifer has been identified as contributing indirect recharge to the basal lens (Tillman et al., 2014). The high-level water found in wells above roughly 400m in elevation in Keauhou Aquifer has been shown to contain recharge that originates from the slopes of Mauna Loa (Fackrell, 2016). The fraction of this high-level aquifer endmember (-6.97‰) was also calculated using a two-endmember mixing line (Fackrell, 2016). Assuming that there is a recharge contribution from both Hualalai (which supplies water to the basal lens) and Mauna Loa (which supplies the high-level water), the indirect recharge from the high-level aquifer would account for 42% of the total recharge to the North Keauhou Group. This agrees with samples taken in the area by Tillman et al. (2014) and Fackrell (2016), though their amounts of indirect recharge were more variable in comparison to this study that used an averaged isotopic signature for the area.

Central Keauhou Group

The integrated recharge paths for the Central Keauhou Group were calculated for both the direction of Hualalai and Mauna Loa to inspect the resulting $\delta^{18}O$ values. It appears that both of these volcanic slopes could contribute recharge to the Central Keauhou Group. The SGD $\delta^{18}O$ value is reached even with a trajectory purely leading to Hualalai to a recharge elevation of only 1000 m. Such an elevation, combined with previous research performed by Tillman et al. (2014), suggests that the high-level aquifer has been contributing water to the basal lens. Therefore, it would seem that some of the recharge contribution is coming from the high level aquifer, which can be fed by Mauna Loa slopes, as also suggested by Fackrell (2016).

South Keauhou Group

For the South Keauhou Group, as with the North Kiholo and North Keauhou groups, the calculated integrated $\delta^{18}O$ values never matched those observed in SGD, despite carrying out the calculations (Equation 5) to the highest elevations of Hualalai and Mauna Loa. The Hualalai path does not seem as realistic as the path from Mauna Loa due to the distance and indirect path relative to elevation contour lines. Therefore, it seems that the South Keauhou Group gets most of its recharge from Mauna Loa. Yet, even the Mauna Loa recharge path alone does not match the SGD sample $\delta^{18}O$, and because the high-level aquifer groundwater is sourced from the flanks of Mauna Loa, indirect recharge from the high level aquifer would not contribute a different isotopic signature. Therefore, either indirect recharge from deeper layers or fog drip may be playing a role in contributing highly negative $\delta^{18}O$ to the SGD sample signature. Fog is isotopically enriched compared to rainfall and causes recharge elevations to be plotted lower than their true altitude, which in turn predicts an integrated recharge path that originates higher than actually observed (Scholl et al., 1996; Kelly and Glenn, 2015). The integrated recharge path $\delta^{18}O$ value never matched that of the samples, despite being carried out to the top of Mauna Loa (4000m). This suggests that fog drip contributes to the aquifer recharge in this area.

Aquifer Catchment Areas

Using the assumed integrated recharge elevations and potential groundwater flow pathways that were outlined above, catchment areas were mapped for each SGD group. These catchment areas define the rough recharge boundaries for each group (Figure 1.8). The extent of these areas was not possible to define in every case because we were limited by sampling

constraints (access to central Kiholo watershed coastline was not possible). The boundary between the North Kiholo and Keauhou-Kiholo Boundary regions was therefore set based on findings of Fackrell (2016). The extent of the South Keauhou group in the southern direction is also unknown and arbitrarily extended to the aquifer boundary.

The North Kiholo Group catchment area is the largest 269 km^2. The North Keauhou catchment area is the second largest at 130 km^2, followed by the Kiholo-Keauhou Boundary catchment area (90 km^2), the Central Keauhou catchment area (87 km^2), and finally the South Keauhou catchment area (36 km^2). At the southern end of Keauhou Aquifer SGD springs were identified based off of TIR imaging, yet their SGD rates were not reported. Upon inspection in the field, we were unable to locate a groundwater influence in these areas. Therefore, these plumes should be studied more closely to better define the South Keauhou catchment area in particular.

Exact groundwater flow paths are not possible to determine, but based on the mapped catchment areas we can analyze the relative recharge contributions to the aquifer from the different parts of the aquifer (Figure 1.8).

For the North Kiholo group, about 37% of the water that discharges as SGD originates as recharge within the Kiholo Aquifer boundary. Indirect recharge from higher aquifers accounts for 63% of all of the recharge needed to reconstruct the coastal $\delta^{18}O$, with results suggesting that all of this upstream recharge originates within the Humuula Saddle region, though the possibility of recharge contributions from Mauna Loa and Mauna Kea cannot be ruled out.

At the Kiholo-Keauhou Boundary, with isotopic measurement uncertainties taken into account, it was determined that 100% of the recharge to coastal springs originates along a flow path leading upslope to the top of Hualalai.

For the North Keauhou group, as mentioned above, there is a 42% recharge influence coming from the slopes of Mauna Loa and feeding into the high-level aquifer. This suggests that only 58% of coastal groundwater discharge originates within the Keauhou Aquifer boundary. Of this 58%, 33% is sourced from below the water level divide, while 25% is sourced from the higher slopes of Hualalai.

In Central Keauhou, our results confirm that there is a connection between the basal lens and high level groundwater in order to reconstruct $\delta^{18}O$ values measured in SGD (Tillman et al., 2014; Kelly and Glenn, 2015, Fackrell, 2016). Specifically, 39% of water discharging as SGD is recharged directly to the basal lens, while 61% is contributed by the high-level aquifer. The data does not allow us to distinguish the source of the recharge to the high level aquifer, only that it seems to originate at a relatively low altitude of 1000 m or lower.

In South Keauhou, 9% of recharge originates at elevations below the basal-high level water divide, leaving 32% to be recharged from above the divide. In total, the recharge within the confines of Keauhou Aquifer only accounts for 41% of the total recharge to SGD springs at the coastline. The rest (59%) must originate from outside the aquifer either as interaquifer flow or from an upstream source, such as the higher slopes of Mauna Loa.

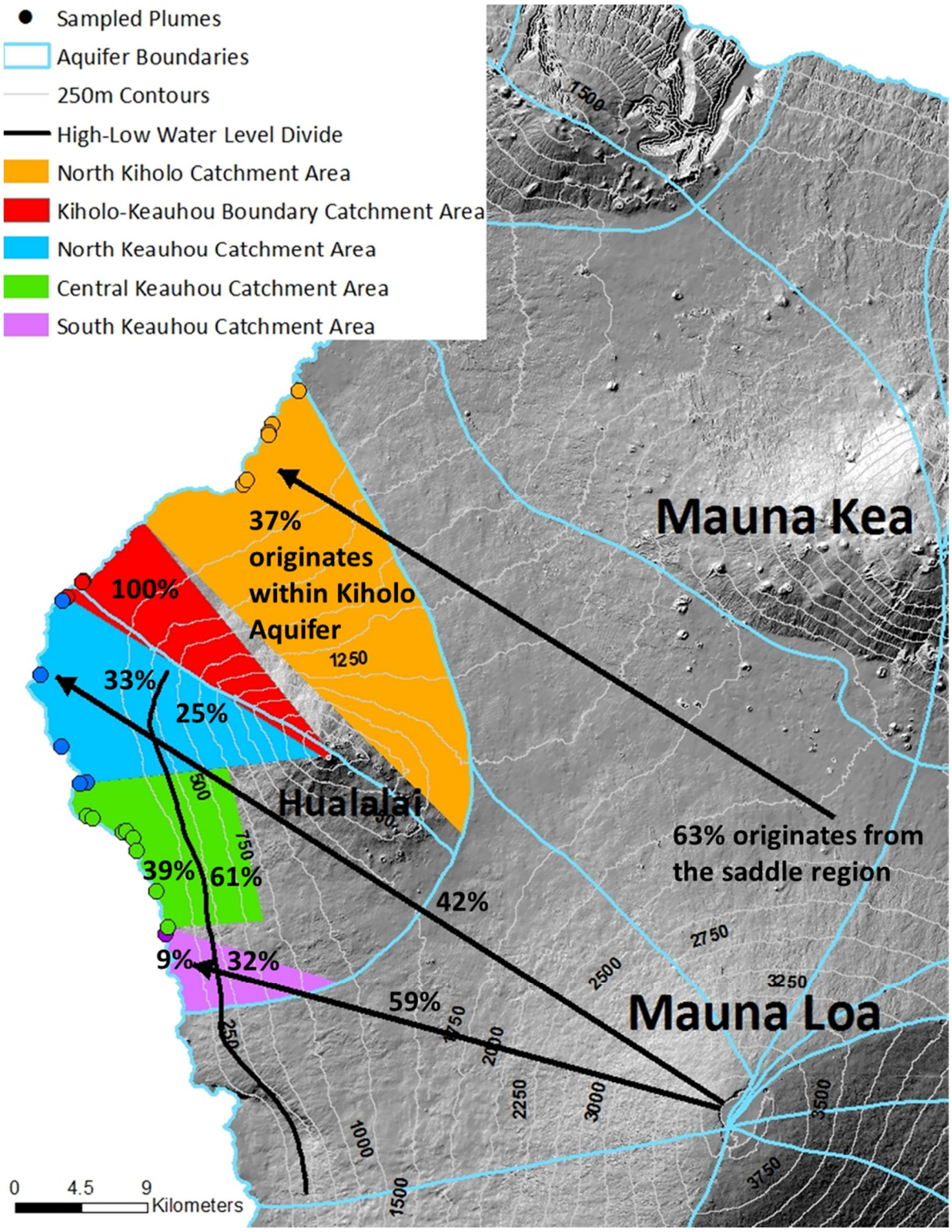

Figure 1.8 Depiction of the catchment areas for each colored group based on their potential integrated recharge pathways. Percentages indicate the amount of recharge originating from each area of the catchment as suggested by SGD $\delta^{18}O$ signatures.

Recharge and Discharge Comparison

In Kiholo Aquifer, recharge (92,347 m^3/d) is far lower than the fresh nearshore SGD rate (147,003 m^3/d). Especially when pumping (34,010 m^3/d) is taken into consideration, it would not be possible for all of the recharge in Kiholo Aquifer to account for all of the discharge.

In Keauhou Aquifer, recharge (335,985 m^3/d) is significantly higher than the fresh nearshore SGD rate (27,301 m^3/d). With a pumping rate of only 55,167 m^3/d, that still leaves 253,517 m^3/d unaccounted for. Some of this discrepancy stems from the plumes that had been identified as areas of groundwater discharge in the central and south Keauhou groups, yet had no discharge rate associated with them. Another possibility is the presence of deeper groundwater flow paths that result in offshore SGD (Oki, 2015). Oki (2015) provided evidence of such deep flow paths based on salinity and temperature data in some wells.

The individual groups, as defined above, were studied in more detail to assess their recharge-discharge water volume balance. Each catchment area was defined based on the distance along the shoreline, the isotopic similarity of the SGD signatures, and the distance land-ward, which was based on recharge elevations derived from recharge pathways that matched SGD $\delta^{18}O$ signatures. Recharge to the different sectors delineated in this way was calculated from GIS recharge maps (Engott, 2011). In the Central Keauhou group, recharge from within the aquifer was able to explain the observed SGD $\delta^{18}O$ signatures, so only recharge within the aquifer was considered. Recharge elelvations in the North Kiholo, Kiholo-Keauhou Boundary, North Keauhou, and South Keauhou, however suggest recharge contributions from outside of the respective aquifer areas. We use the recharge amount in each group and SGD

estimates (Table 1.1) to estimate the recharge-discharge volume balance (Table 1.5). In the North Kiholo group, recharge within the aquifer is not sufficient to provide enough water to match SGD and this supports the result suggested by the isotopes that recharge from upstream aquifers contribute water to SGD. However, if we consider the full recharge area delineated on the basis of recharge elevations, which would include some area between Mauna Loa and Mauna Kea, there is excess water in the aquifer which must be channeled to neighboring aquifers or discharge offshore. Previous research (Tillary and El-Kadi, 2012) suggests that some of the Kiholo Aquifer recharge is channeled by a subsurface structural boundary extending from the summit of Hualali to Puu Anahulu. This water would then discharge in Anaeho'omalu Aquifer. The recharge to other groups also suggests a significant imbalance, all resulting in excess recharge in comparison to SGD. Only the Kiholo-Keauhou Boundary group had excess recharge when compared to the SGD and pumping rates. SGD is only 27-87% of recharge into the other four of the individual sections of the aquifer (Table 1.5). This can only partially be explained by missing SGD rates in the Central and South Keauhou groups.

There are two potential explanations to describe the excess recharge: 1) a deeper flow path may discharge the submarine groundwater further offshore, or 2) lateral flow to neighboring aquifers must be present. It has long been assumed that there are deeper confining layers that trap and contain fresh groundwater before directing it to discharge further offshore (Knee et al., 2008; Bratton, 2010; Knee et al., 2010; Dimova et al., 2012). Bratton (2010) expands on this and has defined SGD on three distinct spatial scales: 1) the nearshore scale, spanning 0-10m offshore, 2) the embayment scale, spanning 10m-10km offshore, and 3) the shelf scale, spanning greater than 10km and including the width and thickness of the

aquifers of the continental shelf. While the latter is specific to continental slopes, subsurface geological structures in Hawaii may create similar hydrological settings.

Evidence of these deep confined layers of freshwater below saltwater-saturated layers in other areas of the Big Island support this theory (Stolper et al., 2009). Specifically, while drilling deep monitoring wells in 2010 about two miles south of Honokohau Harbor at an elevation above 700ft and within the high-level aquifer, a well drilled to a depth of 1760ft below sea level in the basal lens encountered freshwater below brackish-to-salty water. This provides strong evidence that poorly permeable layers trap freshwater at deeper depths. It also provides evidence that at least some of the high-level water does not drain directly into the basal lens, but rather passes beneath it and gets directed further offshore before discharging (Duchesne, 2013). Talks of developing artesian wells to tap into this freshwater zone have been considered, yet more research is needed to determine if this would reduce SGD to coastal ecosystems. These deeper layers of freshwater have large impacts on the management and allocation of freshwater resources in the Keauhou Aquifer and must therefore be better characterized before any action is taken (Duchesne, 2013).

Group	Recharge Within Aquifer Boundaries (m^3/d)	Total Recharge (m^3/d)	SGD (m^3/d)	Pumping (m^3/d)	Percent Discharge (%)
North Kiholo	57,856±14,181	156,367±38,327	131,524±20,655	3,961±446	87
Kiholo-Keauhou Boundary	26,165±4,782	26,165±4,782	17,620±2,496	27,853±1,301	174
North Keauhou	49,855±16,567	85,958±28,563	18,924±5,695	19,232±272	44
Central Keauhou	80,913±15,159	80,913±15,159	10,784±4,732	13,491±3,899	27
South Keauhou	49,941±15,086	122,841±24,369	12,253±5,377	3,437±326	31

Table 1.5 Comparison of recharge and discharge rates for each catchment area.

*SGD extrapolated for springs without measured discharge rates

Another discrepancy in the water budget stems from a significant area upstream of the Central Keauhou group, which contains 47,140 m^3/d of recharge (Figure 1.8). Based on the SGD isotopic signatures, this region could be assigned as recharge to any of the groups in the aquifer except the Central Keauhou group. Therefore, recharge from this region may be flowing to the North Keauhou or South Keauhou groups. But evidence from deep monitoring wells in the area as described above, suggests that freshwater may also be channeled to deeper layers in the aquifer and discharging as offshore SGD (Table 1.5).

Information Derived for Water Management

The definition of groundwater sustainable yield on tropical islands is based on the prevention of seawater intrusion and resulting salinization of pumping wells in the aquifer (Alley et al., 1999). However, it has been suggested that such criteria are insufficient in the sustainable management of groundwater resources, which also supply fresh and brackish water (and the necessary nutrients they carry to sustain aquatic ecosystems) to streams, coastal ponds, and the coastline as well (Duchesne, 2013). The recharge budgets derived in this study can be used to evaluate how pumping from the basal lens and high-level aquifers would affect fresh SGD.

This study only focuses on fresh SGD, as saline SGD is driven by processes other than the hydraulic gradient between the aquifer and the ocean, such as waves, density, currents, and tidal action (Knee et al., 2008; Dulai et al., 2015). If we consider the recharge budgets of the North, Central, and South Keauhou groups, we can conclude that groundwater withdrawal from the pumping of the basal lens should affect the magnitude of fresh SGD proportionally.

Withdrawal from the high-level aquifer will leave 33%, 39%, and 9% of recharge to the basal lens unaffected in the North, Central, and South Keauhou groups, respectively, as those fractions are recharged directly into the basal lens. Therefore, groundwater withdrawal from both the high-level aquifer and the basal lens can potentially directly reduce nearshore SGD, depending on water levels within the basal and high-level regions. Also, as is the case for the North Kiholo, North Keauhou, and South Keauhou group, SGD relies on recharge from an upstream aquifer, be it from the slopes of Mauna Loa or Mauna Kea or from the saddle region between them. Therefore, SGD could be affected by pumping in the neighboring upstream aquifers as well.

Conclusions:

The goal of this study was to identify groundwater recharge areas within the Hualalai aquifers on the Kona Coast of the Big Island, Hawaii. We determined these flow paths by measuring the oxygen isotopes of groundwater at coastal springs and used those values to trace the recharge areas of the groundwater. This in turn allowed us to determine the possible catchment areas for each group of SGD springs. We then projected possible groundwater flow paths from the areas of recharge to the points of discharge at the coastline, and then compared recharge and discharge rates for each catchment area.

While the exact flow paths of groundwater within these aquifer cannot be determined using this method, we identified five separate possible water recharge patterns within the two aquifers, some of which span outside of the aquifer boundaries. In the north Kiholo Aquifer,

isotopic characteristics of SGD suggest that only about 37% of water originates from recharge within the Kiholo Aquifer, which is also supported by the water mass balance of SGD discharge-recharge volume within north Kona. Findings also suggest that, despite geological barriers, SGD signatures are very similar across the Kiholo-Keauhou boundary, implying similar recharge areas and flow paths. In Keauhou Aquifer, recharge to the basal lens makes up only 9-39% of SGD, the rest of the water is sourced from the high-level aquifer. In the case of South Keauhou, the SGD signature suggests 59% of recharge is contributed from elevations beyond the aquifer boundary. This study concludes that there are complex recharge and flow patterns in the Hualalai aquifers, suggesting the occurrence of recharge from neighboring upstream aquifers and lateral flow to adjacent neighboring aquifers.

This study was not able to quantify the exact recharge-discharge water balance due to missing SGD values in the south Keauhou Aquifer. This study also implied that some recharge is channeled to deeper aquifer layers and perhaps discharges farther offshore. However, quantification of such amounts was not possible. Nevertheless, the study confirmed past findings and provided new insight into the interconnectivity of the aquifers in the Hualalai region.

This study contributes new knowledge about the interconnectivity of the aquifers, identifies boundaries based on changes in isotopic signatures and recharge paths that may have some hydrogeological basis. These results can be used for assessing the water budget of the West Hawaii study area and help build on previous works to create an essential baseline for assessing Hawaii's water future security.

However, more research is needed, specifically to deploy a wider topographic range of precipitation collectors to confirm the LMWL for the West Hawaii study area and capture signatures from individual storms, fog and vog drip, as well as fractionation during recharge. More measurements of SGD rates at both previously identified and yet-to-be identified springs are needed to gain a better understanding of the water budget. Additional geochemical analyses, such as dating, and geophysical techniques are called for to further reach definite answers regarding aquifer connectivity, subsurface structures, and deep offshore SGD.

Acknowledgements

I thank my advisor, Henrietta Dulai, for all of her guidance and support. I would also like to thank my committee members, Aly El-Kadi and Nicole Lautze, for all of their insight and feedback. It would not have been possible to complete this project without the dedication, guidance, and assistance of these people.

I would like to thank Trista McKenzie and Eric Welch for helping me with the laboratory work. I thank Brytne Okuhata, Diamond Tachera, Sheree Watson, and Kiana Frank for help with planning and executing fieldwork and sample collection. I thank Natalie Wallsgrove at the University of Hawai'i Stable Isotope Biogeochemistry Lab for processing my samples. I would also like to thank my 'Ike Wai mentor, Daniela Bottjer-Wilson, for all of her support. I also thank fellow students and mentors who were there to support me including Daniel Dores, Michael

Mathiousdakis, U'i Au, Aida Arik, Kilika Bennett, Ku'i Keliipuleole, Barb Bruno, Jenny Engels, Deborah Eason, Scott Rowland, Chip Fletcher, and the entire 'Ike Wai team.

Support for the Hawai'i EPSCoR Program is provided by the National Science Foundation's Research Infrastructure Improvement (RII) Track-1: 'Ike Wai: Securing Hawaii's Water Future Award # OIA-1557349. Any opinions, findings, and conclusions or recommendations expressed in this material are those of the author(s) and do not necessarily reflect the views of the National Science Foundation.

Finally, I would like to thank my family and friends who have shown me support and love throughout my academic journey.

References:

Adams, W. M., Peterson, F. L., Mathur, S. P., Lepley, L. K., Warren, C., & Huber, R. D. (1971). A Hydrogeophysical Survey Using Remote-Sensing Methods from Kawaihae to Kailua-Kona, Hawaii. *Groundwater*, *9*(1), 42–50.

Alley, W. M., Reilly, T. E., & Franke, O. L. (1999). Sustainability of Ground-Water Resources, U.S. Geological Survey Circular 1186. *U.S. Geological Survey Circular 1186*, 79.

Amato, D. W., Bishop, J. M., Glenn, C. R., Dulai, H., & Smith, C. M. (2016). Impact of submarine groundwater discharge on marine water quality and reef biota of Maui. *PLoS ONE*, *11*(11), 1–28.

Bauer, G. R. (2003). A study of the ground-water conditions in North and South Kona and South Kohala Districts, Island of Hawaii, 1991–2002, (Report No. PR-2003-1), 95 p. Retrieved from http://hawaii.gov/dlnr/cwrm/publishedreports/PR200301.pdf

Bratton, J. F. (2010). The Three Scales of Submarine Groundwater Flow and Discharge across Passive Continental Margins. *The Journal of Geology*. https://doi.org/10.1086/655114

Burnett, W.C., Dulaiova, H., 2003. Estimating the dynamics of groundwater input into the coastal zone via continuous radon-222 measurements. Journal of Environmental Radioactivity, 69(1-2): 21-35.

Cable, Jaye E., Burnett, William C., Chanton, Jeffrey P., Weatherly, Georges L. (1996). Estimating groundwater discharge into the northeastern Gulf of Mexico using radon-222. Earth and Planetary Science Letters, 144 (3-4), 591-604.

Clague and Langenheim. (1987). *Volcanism in Hawaii*. (R. Decker, T. Wright, & P. Stauffer, Eds.), *U.S. GEOLOGICAL SURVEY PROFESSIONAL PAPER 1350*. https://doi.org/10.1016/0003-6870(73)90259-7

Dimova, N. T., Swarzenski, P.W., Dulaiova, H., Glenn, C.R. 2012. Utilizing multichannel electrical resistivity methods to examine the dynamics of the fresh water–seawater interface in two Hawaiian groundwater systems, Journal of Geophysical Research 117 (C2), C02012

Duarte, T.K., Hemond, H.F., Frankel, D., Frankel, S., 2006. Assessment of submarine groundwater discharge by handheld aerial infrared imagery: case study of Kaloko fishpond and bay, Hawaii. Limnology and Oceanography: Methods, 4(7): 227-236.

Duchesne, T. A. (2013). Petition to Designate the Keauhou Aquifer System a Water Management Area.

Dudley, B.D. et al., 2014. Influences of N-Fixing and Non-N-Fixing Vegetation and Invasive Fish on Water Chemistry of Hawaiian Anchialine Ponds1. Pacific Science, 68(4): 509-523.

Dudley, B. D., Hughes, R. F., Baldwin, J., Miyazawa, Y., Dulai, H., Waters, C., … Giambelluca, T. (n.d.). Phreatophytic tree invasion along dry leeward coasts of Hawaii Island; using a LiDAR-derived isoscape to assess hydrologic impact.

Dulai, H., Kamenik, J., Waters, C., Kennedy, J., Babinec, J., Jolly, J. Williamson, M., 2016. Autonomous long-term gamma-spectrometric monitoring of submarine groundwater discharge trends in Hawaii. Journal of Radioanalytical and Nuclear Chemistry. 10.1007/s10967-015-4580-9.

DURRIDGE Company Inc. (2011). RAD H20 User Manual, (978), 1–29.

Engott, J.A., 2011. A water-budget model and assessment of groundwater recharge for the Island of Hawai'i: U.S. Geological Survey Scientific Investigations Report 2011-5078, 53 p.

ESRI 2016. ArcGIS Desktop: Release 10.5. Redlands, CA: Environmental Systems Research Institute.

Fackrell, J.K. Geochemical evolution of Hawaiian groundwater. Thesis. University of Hawaii at Manoa, 2016.

Fackrell, J.K., and Glenn, C.R., 2014. How much do high-level aquifers impact SGD and the coastal zone in Hawai‘i? Unscrambling the mix with water isotopes. February 23–28, 2014 Ocean Science Meeting, Honolulu, HI.

Glenn, C. R., Whittier, R. B., Dailer, M. L., Dulaiova, H., El-kadi, A. I., Fackrell, J., & Sevadjian, J. (2013). Lahaina Groundwater Tracer Study, 502.

Godoy, J.M., Godoy, M. L., Neto, A., 2012. Direct determination of δ(D) and δ(18O) in water samples using cavity ring down spectrometry: Application to bottled mineral water. Journal of Geochemical Exploration 119–120: 1–5.

Gregg, C. E., Houghton, B. F., Johnston, D. M., Paton, D., & Swanson, D. A. (2004). The perception of volcanic risk in Kona communities from Mauna Loa and Hualālai volcanoes, Hawai'i. *Journal of Volcanology and Geothermal Research*, *130*(3–4), 179–196. https://doi.org/10.1016/S0377-0273(03)00288-9

Hoover, D. J., & MacKenzie, F. T. (2009). Fluvial fluxes of water, suspended particulate matter, and nutrients and potential impacts on tropical coastal water Biogeochemistry: Oahu, Hawai'i. *Aquatic Geochemistry*, *15*(4), 547–570.

Hunt, C. (2008). Results of Sampling for Wastewater Tracers At and Near Kealakehe WWTP, Kona,Hawaii.

Ike Wai Project Description. (2015).

Johnson, A. (2008). *Groundwater Discharge From the Leeward Half of the Big Island, Hawaii*. University of Hawaii at Manoa.

Johnson, A.G., Glenn, C.R., Burnett, W.C., Peterson, R.N., Lucey, P.G., 2008. Aerial infrared imaging reveals large nutrient-rich groundwater inputs to the ocean. Geophysical Research Letters, 35(15).

Kelly, J. L., & Glenn, C. R. (2015). Chlorofluorocarbon apparent ages of groundwaters from west Hawaii, USA. *Journal of Hydrology*, *527*, 355–366. https://doi.org/10.1016/j.jhydrol.2015.04.069

Knee, K.L.S., J.H.; Grossman, E.E.; and Paytan, A., 2008. Submarine ground water discharge and fate along the coast of Kaloko-Honokohau National Historical Park, Hawaii-Part 2, Spatial and

Temporal Variations in Salinity, Radium-Isotope Activity, and Nutrient Concentrations in Coastal Waters, December 2003-April 2006: U.S. Geological Survey Scientific Investigations Report 2008-5128, 31 p.

Knee, K.L., Street, J.H., Grossman, E.E., Boehm, A.B., Paytan, A., 2010. Nutrient inputs to the coastal ocean from submarine groundwater discharge in a groundwater-dominated system: Relation to land use (Kona coast, Hawaii, U.S.A.). Limnology and Oceanography, 55(3): 1105-1122.

Knee, K. L., Crook, E. D., Hench, J. L., Leichter, J. J., & Paytan, A. (2016). Assessment of Submarine Groundwater Discharge (SGD) as a Source of Dissolved Radium and Nutrients to Moorea (French Polynesia) Coastal Waters. *Estuaries and Coasts*, *39*(6), 1651–1668.

Kwon, E. Y., Kim, G., Primeau, F., Moore, W. S., Cho, H.-M., Devries, T., … Cho, Y.-K. (2014). Global estimate of submarine groundwater discharge based on an observationally constrained radium isotope model. *Geophysical Research Letters*, 1–7. https://doi.org/10.1002/2014GL061574

Lane-Smith, D. R., W. C. Burnett, and H. Dulaiova, 2002. Continuous Radon-222 Measurements in the Coastal Zone, *Sea Technology* October 2002, 37-45.

McMurtry, G.M., Fan, P.-F., Coplen, T.B., 1977. Chemical and Isotopic Investigations of Froundwater in Potential Geothermal Area in Hawaii. Am. J. Sci. 277, 438–458.

Moore, R. B., Clague, D. A., Rubin, M., & Bohrson, W. A. (1987). Volcanism in Hawaii. In R. Decker, T. Wright, & P. Stauffer (Eds.), *U.S. GEOLOGICAL SURVEY PROFESSIONAL PAPER 1350* (pp. 571–609). https://doi.org/10.1016/0003-6870(73)90259-7

Moore, W.S 1996. Large groundwater inputs to coastal waters revealed by 226Ra enrichments. Nature, 380.

Moore, W.S., 1998. The subterranean estuary: a reaction zone of ground water and sea water. Marine Chemistry, 65: 111-125.

Nelson, C. E., Donahue, M. J., Dulaiova, H., Goldberg, S. J., La Valle, F. F., Lubarsky, K., … Thomas, F. I. M. (2015). Fluorescent dissolved organic matter as a multivariate biogeochemical tracer of submarine groundwater discharge in coral reef ecosystems. *Marine Chemistry*, *177*(2015), 232–243.

Oki, D.S., 1999. Geohydrology and Numerical Simulation of the Ground-Water Flow System of Kona, Island of Hawaii.

Oki, D.S., 2015. Unravelling the role of deep groundwater circulation on the coastal freshwater-lens system, Kona, Hawaii Island, Water Resource Sustainability Issues on Tropical Islands, December 1−3, 2015, Honolulu, Hawai'i.

Oram, B. (2014). Radon in Water, Air, and Soil. Retrieved February 4, 2018, from https://www.water-research.net/index.php/radon

Peterson, D. W., & Moore, R. B. (1987). Geologic History and Evolution of Geologic Concepts, Island of Hawaii. In *Volcanism in Hawaii* (pp. 149–189).

Peterson, R.N., Burnett, W.C., Glenn, C.R., Johnson, A.G., 2009. Quantification of point-source groundwater discharges to the ocean from the shoreline of the Big Island, Hawaii. Limnology and Oceanography, 54(3): 890-904.

Prouty, N. G., Swarzenski, P. W., Fackrell, J. K., Johannesson, K., & Palmore, C. D. (2017). Groundwater-derived nutrient and trace element transport to a nearshore Kona coral

ecosystem: Experimental mixing model results. *Journal of Hydrology: Regional Studies*, *11*, 166–177. https://doi.org/10.1016/j.ejrh.2015.12.058

Sawyer, A.H., David, C.H., Famiglietti, J.S., 2016. Continental patterns of submarine groundwater discharge reveal coastal vulnerabilities. Science, 353(6300): 705-7.

Scholl, M. A., Ingebritsen, S. E., Janik, C. J., & Kauahikaua, J. P. (1996). Use of precipitation and groundwater isotopes to interpret regional hydrology on a tropical volcanic island: Kilauea volcano area, Hawaii. Water Resources Research, 32(12), 3525–3537.

Scholl, M. A., Gingerich, S. B., & Tribble, G. W. (2002). The influence of microclimates and fog on stable isotope signatures used in interpretation of regional hydrology: East Maui, Hawaii. *Journal of Hydrology*, *264*(1–4), 170–184. https://doi.org/10.1016/S0022-1694(02)00073-2

Slomp, C. P., & Van Cappellen, P. (2004). Nutrient inputs to the coastal ocean through submarine groundwater discharge: Controls and potential impact. *Journal of Hydrology*, *295*(1–4), 64–86.

Stearns, H.T., MacDonald, G.A., 1946. Geology and ground-water resources of the island of Hawaii. United States Geological Survey Hawai'i Division of Hydrography Bulletin 9.

Street, J.H., K.L. Knee, E.E. Grossman, and A. Paytan. 2008. Submarine groundwater discharge and nutrient addition to the coastal zone and coral reefs of leeward Hawaii. Marine Chemistry, 109: 355–376.

Stolper, Edward M., et al. "Deep Drilling into a Mantle Plume Volcano: The Hawaii Scientific Drilling Project." Scientific Drilling, vol. 7, 24 Mar. 2009, doi:10.2204/iodp.sd.7.02.2009.

Tillery, S, El-Kadi, A. 2012. Conceptual model for Kiholo Bay watershed and Kaloko-Honokohau National Historical Park, Hawaii.

Tillman, F. D., Oki, D. S., Johnson, A. G., Barber, L. B., & Beisner, K. R. (2014). Investigation of geochemical indicators to evaluate the connection between inland and coastal groundwater systems near Kaloko-Honokōhau National Historical Park, Hawai'i. Applied Geochemistry, 51, 278–292.

Waters, C.A., 2015. Variability in submarine groundwater discharge composition and the fate of groundwater delivered nutrients at Kiholo Bay and Honokohau Harbor, North Kona District, Hawaii, University of Hawaii at Manoa, 1590 pp.

1976 Digital GIRAS (Geographic Information Retrieval and Analysis) files, Hawaii Statewide GIS Program, Office of Planning / Download GIS Data. State of Hawaii, n.d. Web. 15Sept. 2017.

Appendix:

Table A.1 Raw geochemistry data from each spring, including data from sites samples multiple times. Samples are listed according to sampled date and time.

Sample Name	Latitude	Longitude	Date	Time	Temperature (Celsius)	Specific Conductance (mS/cm)	Salinity	pH	Dissolved Oxygen (Saturation %)	Dissolved Oxygen (mg/l)	$\delta^{18}O$ (‰)	Standard Deviation $\delta^{18}O$ (‰)	$\delta^{2}H$ (‰)	Standard Deviation $\delta^{2}H$ (‰)
OKA1	19.64282	-156.00969	11/13/16	15:03	26.19	51.60	33.89	8.19	115.50	7.70	0.40	0.26	3.50	0.39
OKA2	19.64282	-156.00969	11/13/16	20:31	24.09	47.89	31.20	7.94	68.30	4.78	-0.10	0.10	1.60	0.24
OKA3	19.64282	-156.00969	11/14/16	4:50	24.88	52.28	34.42	7.98	100.00	6.80	0.40	0.03	3.80	0.64
OKA4	19.64282	-156.00969	11/14/16	9:35	25.69	58.60	31.68	8.25	153.70	10.48	-0.20	0.02	1.10	0.33
KBA1	19.85544	-155.92295	11/14/16	15:05	24.98	45.42	29.42	7.94	103.00	7.22	-0.60	0.03	-2.90	0.01
KBA2	19.85544	-155.92295	11/14/16	18:02	23.96	38.75	24.97	8.08	94.50	6.90	-2.50	0.04	-15.90	0.62
KBA3	19.85544	-155.92295	11/14/16	21:30	22.21	21.30	12.70	7.86	84.50	6.85	-6.10	0.10	-41.70	0.51
KBA4	19.85544	-155.92295	11/15/16	1:00	23.35	43.77	28.50	7.75	94.20	6.86	-1.50	0.07	-9.40	0.29
KBA5	19.85544	-155.92295	11/15/16	4:54	23.45	51.91	34.18	7.88	99.90	5.91	0.20	0.09	2.10	0.78
KBA6	19.85544	-155.92295	11/15/16	7:41	24.37	51.15	33.60	7.90	101.80	7.02	-0.10	0.08	-0.70	0.38
KBA7	19.85544	-155.92295	11/15/16	11:35	24.40	32.48	19.91	8.02	113.90	8.47	-3.90	0.11	-25.50	0.66
KBB1	19.85855	-155.92062	11/14/16	16:00	24.36	38.25	24.30	7.99	101.80	7.42	-2.30	0.05	-13.60	0.40
KBB3	19.85855	-155.92062	11/14/16	20:44	21.94	25.29	15.46	8.26	70.50	5.52	-4.30	0.04	-29.80	0.52
KBB5	19.85855	-155.92062	11/15/16	4:00	23.22	39.23	25.04	7.89	84.30	6.23	-1.70	0.10	-12.00	0.17
KBB7	19.85855	-155.92062	11/15/16	10:38	24.31	43.35	28.26	7.63	91.20	6.49	-3.00	0.02	-20.10	0.14
HHA1	19.66926	-156.02108	11/15/16	15:46	17.92	30.36	16.86	7.31	76.80	6.56	-0.70	0.12	-4.60	0.50
HHA2	19.66926	-156.02108	11/15/16	19:08	1.48	27.37	16.82	7.59	74.80	6.55	-1.00	0.04	-6.40	0.31
HHA3	19.66926	-156.02108	11/15/16	21:41	18.06	34.74	21.13	7.69	72.60	6.28	-2.10	0.12	-10.60	0.47
HHA5	19.66926	-156.02108	11/16/16	4:52	20.83	41.17	26.73	7.73	79.80	6.05	-0.30	0.09	-1.80	0.38
HHA6	19.66926	-156.02108	11/16/16	8:36	21.18	38.15	24.41	7.86	82.70	6.34	-1.60	0.12	-7.80	0.28
HHA7	19.66926	-156.02108	11/16/16	11:50	19.06	31.73	20.98	7.18	78.10	6.39	-2.20	0.02	-10.90	0.51
HHB1	19.66853	-156.02547	11/15/16	16:24	24.13	45.62	29.39	7.69	94.10	6.71	-0.40	0.12	-1.70	0.24
HHB3	19.66853	-156.02547	11/15/16	22:05	20.94	38.37	22.85	7.67	77.40	6.03	-1.20	0.06	-6.10	0.17
HHB5	19.66853	-156.02547	11/16/16	5:20	22.74	44.52	29.00	7.85	84.30	6.18	-0.70	0.04	-3.50	0.28
HHB7	19.66853	-156.02547	11/16/16	11:28	21.91	39.82	25.69	7.69	82.70	6.25	-0.50	0.04	-2.40	0.45

Table A.1 Continued

Sample Name	Latitude	Longitude	Date	Time	Temperature (Celsius)	Specific Conductance (mS/cm)	Salinity	pH	Dissolved Oxygen (Saturation %)	Dissolved Oxygen (mg/l)	$\delta^{18}O$ (‰)	Standard Deviation $\delta^{18}O$ (‰)	$\delta^{2}H$ (‰)	Standard Deviation $\delta^{2}H$ (‰)
QLT1	19.64887	-156.02121	05/30/07	16:45	26.50	49.34	32.22	7.65	88.50	5.94	0.10	0.03	1.20	0.06
Heiau 1	19.57699	-155.96798	05/31/17	14:09	20.78	8.16	4.53	7.31	93.70	8.16	-4.40	0.04	-22.80	0.05
Heiau 2	19.57709	-155.96798	05/31/17	14:21	20.96	7.97	4.43	7.25	93.80	8.17	-4.50	0.02	-23.00	0.07
Heiau 3	19.57721	-155.96790	05/31/17	14:54	23.68	11.61	6.63	7.71	90.20	7.36	-4.10	0.01	-21.00	0.04
P1A	19.91392	-155.88759	06/26/17	8:52	24.00	10.56	5.98	7.86	83.40	6.79	-7.40	0.01	-50.20	0.01
P1B	19.91372	-155.88797	06/26/17	9:27	24.11	9.24	5.17	8.12	92.20	7.54	-7.80	0.06	-52.70	0.20
P1C	19.91318	-155.88852	06/26/17	9:54	23.34	14.17	8.21	7.66	95.00	7.72	-7.10	0.01	-48.20	0.09
P6	19.89309	-155.90469	06/26/17	12:42	23.24	9.70	5.46	7.54	98.50	8.17	-7.30	0.03	-49.20	0.17
P8A	19.88796	-155.90671	06/26/17	11:23	24.52	17.86	10.50	7.59	92.60	7.28	-5.50	0.01	-36.30	0.07
P8B	19.88668	-155.90701	06/26/17	11:57	24.58	9.68	5.44	7.71	96.80	7.79	-7.30	0.05	-48.90	0.11
P22A	19.79354	-156.02589	06/25/17	11:21	NA	NA	NA	NA	NA	NA	-2.00	0.01	-10.40	0.08
P22B	19.79274	-156.02695	06/25/17	11:36	26.91	28.69	17.65	7.71	109.20	7.91	-2.40	0.04	-12.50	0.02
P23	19.78330	-156.03651	06/25/17	9:58	NA	NA	NA	NA	NA	NA	-4.30	0.01	-22.30	0.07
P24	19.78172	-156.03958	06/25/17	9:06	22.89	41.10	26.34	7.74	70.80	5.20	-1.20	0.09	-7.40	0.22
P25	19.73564	-156.05302	06/27/17	11:28	24.72	41.74	26.90	7.22	100.50	7.18	-1.10	0.02	-5.80	0.10
PKI1	19.69133	-156.03821	06/27/17	9:43	19.97	24.64	15.06	6.90	88.00	7.28	-3.50	0.02	-20.20	0.05
PKI2	19.69132	-156.03821	06/27/17	10:06	24.22	26.35	16.12	7.11	74.70	5.71	-3.60	0.03	-21.40	0.02
P34	19.64724	-156.01704	06/27/17	8:28	23.95	37.42	23.72	7.80	97.80	7.12	-1.40	0.07	-6.30	0.20
P37	19.63891	-155.99757	06/28/17	9:00	22.37	41.83	26.84	7.66	56.30	4.12	-1.10	0.05	-5.30	0.08
P38	19.63968	-155.99477	06/28/17	9:49	23.11	27.01	16.58	7.11	85.30	6.65	-2.00	0.02	-7.90	0.13
P39	19.63543	-155.99068	06/28/17	10:55	21.90	19.85	11.74	7.95	101.10	8.35	-2.60	0.02	-9.60	0.05
P40	19.62815	-155.98805	08/18/17	6:18	20.52	21.23	12.80	7.82	NA	NA	-1.90	0.01	-9.20	0.07
P41	19.60286	-155.97458	08/18/17	7:37	23.90	42.95	27.65	7.79	NA	NA	-0.70	0.04	-2.90	0.16
P43	19.58107	-155.96680	08/18/17	8:36	23.91	27.43	16.77	8.00	NA	NA	-1.70	0.03	-8.30	0.05

Table A.2 Integrated recharge calculations for different recharge paths leading from the grouped coastal springs upslope to the three main volcanoes.

	Recharge (m^3/d)																	
Elevation Interval (m)	0-250	250-500	500-750	750-1000	1000-1250	1250-1500	1500-1750	1750-2000	2000m-2250	2250-2500	2500-2750	2750-3000	3000-3250	3250-3500	3500-3750	3750-4000	**Aggregated $\delta^{18}O$**	**Sample $\delta^{18}O$**
$\delta^{18}O$ calculated using Equations 3 and 4	-3.42	-3.72	-4.02	-4.32	-4.62	-4.92	-5.22	-6.83	-7.6275	-8.425	-9.2225	-10.02	-10.8175	-11.615	-12.4125	-13.21		
North Kiholo Recharge Path to Hualalai	13.52	11.37	24.72	20.9	14.66	11.15	4.08	3.35	3.87	6.54							**-5.54**	**-8.29**
North Kiholo Recharge Path to Mauna Loa	9.88	9.56	7.15	5.22	10.42	17.97	21.02	10.14	7.8	6.31	4.85	3.72	3.89	3.38	3.83	4.76	**-6.33**	**-8.29**
North Kiholo Recharge Path to Mauna Kea	17.94	9.37	24.75	22.34	12.36	7.95	7.91	6.6	7.07	5.42	5.13	5.53	4.46	5.34	4.28	4.72	**-5.97**	**-8.29**
Kiholo-Keauhou Recharge Path to Hualalai	19.7	21.73	19	17.16	13.27	17.92	11.15	6.94	6.53	0.15							**-4.53**	**-4.86**
Kiholo-Keauhou Recharge Path to Mauna Loa	14.27	5.88	25.46	38.06	46.26	63.3	21.95	12.27	10.46	7.84							**-4.91**	**-4.86**
Kiholo-Keauhou Recharge Path to Mauna Kea	23.99	29.99	14.94	30.63	22.36	12.74	6.79	6.51	8.58	5.58	4.17	5.73	3.86	4.94	4.02	8.47	**-4.86**	**-4.86**
North Keauhou Recharge Path to Hualalai	38.23	55.41	26.9	16.64	14.35	5.89	3.27	2.89	4.47	3.48							**-4.15**	**-5.31**
North Keauhou Recharge Path to Mauna Loa	76.02	52.82	52.81	100.14	151.03	197.15	26.05	10.79	7.87	7.08	6.32	5.93	5.02	5.35	4.78	4.9	**-4.84**	**-5.31**
Central Keauhou Recharge Path to Hualalai	45.47	45.1	35.33	19.84	11.18	10.34	4.62	3.03	3.9	3.46							**-4.72**	**-3.77**
Central Keauhou Recharge Path to Mauna Loa	60.44	45.48	77.94	68.14	166.51	175.15	25.95	10.87	7.66	6.71	6.5	5.78	5.14	5.1	5.1	4.67	**-3.90**	**-3.77**
South Keauhou Recharge Path to Hualalai	26.48	44.75	60	68.26	32.11	15.2	12.16	3.42	2.9	3.2							**-4.56**	**-5.12**
South Keauhou Recharge Path to Mauna Loa	22.38	181.013	87.86	128.43	174.5	100.34	26.53	10.84	7.09	7.13	6.71	5.33	2.45	5.13	4.84	4.88	**-4.66**	**-5.12**